うな病態の不均一性(heterogeneity)が治療難航の一因となっている．現在まで，髄鞘や軸索の再生促進薬はなく，新規の標的分子に対する画期的な創薬が待望されている．

2003年にヒトゲノムの解読が完了し，個々の細胞における全遺伝子や蛋白質の発現を網羅的に解析可能なポストゲノム時代が到来し，創薬研究の中心はゲノム創薬へとパラダイムシフトした．網羅的発現解析を統合したオミックス研究により，がんや神経難病の診断バイオマーカーや治療標的分子がつぎつぎ明らかにされた．同時に薬理ゲノミクスの分野は急成長を遂げ，薬物応答性個人差をある程度予測可能となり，テーラメイド医療(personalized medicine)の樹立に道が開かれた．システム生物学(systems biology)の観点からは，ヒトは大規模な分子ネットワークで精密に構築された複雑系であり，多くの難病がシステム固有の防御機構であるロバストネス(robustness)の破綻に起因すると考えられている．したがって難病の病態解明のためには，オミックス研究に直結したゲノムワイドの分子ネットワーク解析が重要な研究手段となる．

最近，われわれは公共のデータをバイオインフォマティクスの分子ネットワーク解析ツールで再解析し，MSの創薬標的分子を同定することができた[1]．以下にわれわれの研究を中心に，MSの病態解明や治療標的探索を目的とした分子ネットワーク解析について概説する．

1．分子ネットワークの解析方法

生体内では蛋白質は複雑なネットワークから成るシステムを構築している．したがって難病の病態解明のためには，個々の蛋白質の機能解析のみならず，蛋白質が構築している分子ネットワークやネットワークの構成要素であるパスウェイの同定が重要となる．一般的に蛋白質間相互作用(protein-protein interaction：PPI)には，単純な直接的結合関係のみならず，活性化，活性抑制，運搬，酵素反応，複合体形成など多彩な相互作用様式が存在する．複雑多岐のオミックスデータに関連している分子ネットワークを解析するためには，精査された文献情報に裏づけられた専用の解析ツールを使う必要がある．すなわち，膨大な文献情報からさまざまな分子間相互作用を抽出し，信頼性の高い知識を整理してコンテンツとして収録した知識データベース(knowledgebase)を利用して，既知のどのネットワークやパスウェイに最も高い類似性を呈しているかについて，統計学的解析手法を用いて調べる方法である[1]．Web上でフリーに利用できる代表的なknowledgebaseには，Kyoto Encyclopedia of Genes and Genomes (KEGG) (www.kegg.jp)，the Protein Analysis Through Evolutionary Relationships (PANTHER) classification system (www.pantherdb.org)，Search Tool for the Retrieval of Interacting Genes/Proteins (STRING) (string.embl.de)などがある．とくにKEGGとPANTHERは，キュレーターとよばれる専門家によって精査された遺伝子や代謝物の情報を収録している．2011年4月現在，KEGG PATHWAYには392 reference pathwaysから構成される134,607パスウェイが収録されている．また利用価値の高いデータベースとして，DAVID Bioinformatics Resources (david.abcc.ncifcrf.gov)は，網羅的解析で同定した膨大な遺伝子セットのアノテーションを一括しておこなうために開発されたツールである．Functional Annotationツールに目的の遺伝子セットを入力すると，統計学的な検定をおこなって，最も密接に関連しているKEGG pathwayを同定できる．PANTHERでも同様にreference setとの比較により，類似性の統計学的有意差を多重検定で評価できる．STRINGはKEGG，HPRD，BIND，IntActなどの網羅的PPI情報も統合して収録しており，PubMedアブストラクトからは自然言語処理(natural language processing)によるテキストマイニングを介して，分子間相互作用に関する

膨大な情報を収集している．

また分子ネットワーク解析のために樹立された有償ツールとしては，Ingenuity Pathways Analysis (IPA) (Ingenuity Systems, Redwood City, CA) (www.ingenuity.com) や KeyMolnet (Institute of Medicinal Molecular Design, Tokyo) (www.immd.co.jp) などがある．これらは精選された文献を専門家が精読して，分子間相互作用に関する信頼性の高い情報を収集しており，定期的にアップデートされている．KeyMolnet は日本語入力にも対応しており，分子ネットワークの検索法として，結合・発現制御・複合体形成を包括的に調べる周辺検索 (neighboring search)，発現制御に関与する転写因子群を調べる共通上流検索 (common upstream search)，始点と終点間のネットワークを調べる始点終点検索 (N-points to N-points search)，複数の端点を始点として，最多数の始点を含む最小の分子ネットワークを調べる相互関係検索 (interrelation search) を選択できる．

2．MS 脳病巣プロテオーム解析からみた創薬標的分子

2008 年に Han らは 6 例の MS 凍結脳を用いて，病理学的にステージを確認した脳病巣から laser microdissection で採取したサンプルを SDS-PAGE で分離後に，蛋白質を抽出し，トリプシン消化ペプチド断片を質量分析で網羅的に解析した[2]．病理学的ステージは，炎症性細胞浸潤と浮腫を主徴とする急性脱髄巣 (active plaque：AP)，炎症が脱髄巣辺縁部に限局している慢性活動性脱髄巣 (chronic active plaque：CAP)，炎症所見に乏しくアストログリアの瘢痕形成を主徴とする慢性非活動性脱髄巣 (chronic plaque：CP) に分類した．同時に 2 例の健常脳のプロテオームも解析した．その結果，AP から 1082，CAP から 1728，CP から 1514，合計 4324 種類の蛋白質を同定した．さらに INTERSECT プログラムを用いて，健常脳では検出されずかつ各ステージ特異的な蛋白質を選び出し，AP 158，CAP 416，CP 236 種類からなるプロテオームデータを公開した[2]．彼らは PROTEOME-3D を用いてアノテーションを解析し，CAP において血液凝固系蛋白質 SERPINA5 (protein C inhibitor)，F3 (tissue factor)，FN1，THBS1，VTN の発現を認めた．この所見にもとづいて，抗凝固薬である thrombin inhibitor hirudin および activated protein C を用いて，MS 動物モデルであるマウス自己免疫性脳脊髄炎 (experimental autoimmune encephalomyelitis：EAE) を治療した．どちらの抗凝固薬も，抗原特異的リンパ球の増殖と IL-17，TNF-α 産生を抑制した．以上の結果より，血液凝固系蛋白質が新規 MS 創薬標的分子となることが示唆された．しかしながら大多数を占める凝固系以外の蛋白質に関しては，MS 脳分子病態における意義は明らかにされなかった．

われわれは，Han らのデータのプロテオームに関する UniProt ID を，Entrez Gene ID および KEGG ID に変換して，KEGG，PANTHER，IPA，KeyMolnet に入力し，各ステージ特異的プロテオームを最も良く反映している分子ネットワークを同定した[3]．KEGG では，CAP プロテオームと focal adhesion (hsa04510) ($p=5.21E-05$) (**図 1**) および extracellular matrix (ECM)-receptor interaction (hsa04512) ($p=1.25E-04$) との関連性を認めた．PANTHER では，CAP プロテオームと inflammation mediated by chemokine and cytokine signaling pathway ($p=2.63E-03$)，integrin signaling pathway ($p=3.55E-03$)，CP プロテオームと integrin signaling pathway ($p=4.33E-02$) との関連性を認めた．すなわち KEGG と PANTHER の解析から，MS 慢性病巣における ECM-integrin シグナル伝達系の中心的役割が示唆された．KEGG と PANTHER による解析では，AP プロテオームと密接に関連するパスウェイは検出されなかった．

一方 IPA では，AP プロテオームは cellular as-

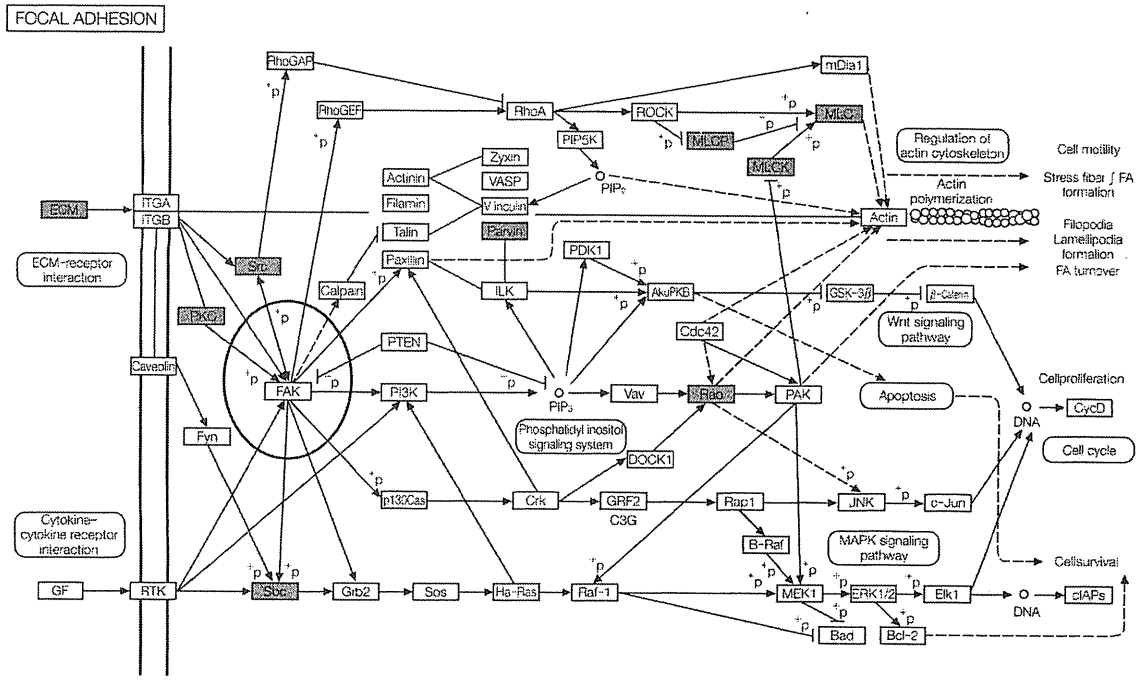

図 1. KEGG による MS 脳病巣 CAP プロテオームの分子ネットワーク解析

KEGG による解析では，MS 脳病巣 CAP プロテオーム(灰色)と focal adhesion (hsa04510：COL1A1, COL1A2, COL5A2, COL6A2, COL6A3, FN1, LAMA1, MYLK, SHC3, PPP1CA, PARVA, PRKCB1, MYL7, RAC3, SPP1, SRC, THBS1, VTN：ECM 構成要素は ECM として一括)との関連性が示唆された．Focal adhesion kinase (FAK)が，ネットワークのハブ(楕円)となることがわかる．

sembly and organization, cancer, and cellular movement (p＝1.00E-49)，CAP プロテオームは dermatological diseases and conditions, connective tissue disorders, and inflammatory disease (p＝1.00E-47)，lipid metabolism, molecular transport, and small molecule biochemistry (p＝1.00E-47)，CP プロテオームは cell cycle, cell morphology, and cell-to-cell signaling and interaction (p＝1.00E-50) との関連性を認めた．CAP プロテオームの dermatological diseases and conditions, connective tissue disorders, and inflammatory disease ネットワークは，BGN, CHI3L1, CNN2, COL1A1, COL1A2, COL6A2, COL6A3, CXCL11, ENTPD1, ERK, FBLN2, FERMT2, FN1, GBP1, HSPG2, Ifn gamma, INPP5D, Integrin, LAMA1, LUM, Mlc, MYL7, MYL6B, NES, P4HA1, Pak, PARVA, POSTN, PRELP, SERPINA5, SERPINH1, Tgf beta, TGFBR3, THBS1, VTN から構成されており，ECM-integrin シグナル伝達系の関与を示唆している．最後に KeyMolnet を用いて，MS 関連 75 分子を始点，ステージ特異的プロテオームの各分子を終点として，始点終点検索で最短経路となるネットワーク解析した．AP プロテオームは IL-4 signaling pathway (p＝1.79E-13)，CAP プロテオームは PI3K signaling pathway (p＝7.25E-18)，CP プロテオームは IL-4 signaling pathway (p＝1.04E-16) と最も密接に関連していた．また CAP と CP は integrin signaling pathway (p＝2.13E-12 および p＝2.57E-12) との関連性も認めた．

以上のように，4 種類の異なるツール KEGG, PANTHER, IPA, KeyMolnet は，さまざまな独

自の分子ネットワークを抽出したが，共通してCAP，CPプロテームにおけるECM-integrinシグナル伝達系の中心的役割を示唆した[3]．Integrinは複数のα，βサブユニットから構成される24種類のヘテロダイマー分子で，ECMのリガンドとしてはたらく．β1 integrinファミリーはcollagen，fibronectin，laminininと結合し，αv integrinファミリーはvitronectinと結合する．ECM-integrin相互作用を介するoutside-in，inside-outシグナルは，細胞骨格の動態制御を介する細胞接着，遊走，分化，増殖にとって必須である．MS脳病巣プロテームで同定したfibronectinやvitronectinは，主として破綻したBBBを通過して脳実質に浸透した血漿成分に由来する．ECM，integrinが著増している慢性病巣においては髄鞘や軸索の再生が著しく乏しい．その理由として，グリア瘢痕に含まれているECM蛋白質自体が髄鞘や軸索の再生阻害因子としてはたらく可能性や，活性化マクロファージやミクログリアが産生する蛋白質分解酵素がECMに結合して長期に保持され，髄鞘の崩壊が遷延化している可能性があげられている[4]．またECM-integrinシグナル伝達系は，リンパ球のホーミングや血管外遊出，アストログリアやミクログリアの活性化，オリゴデンドログリア前駆細胞の分化抑制を介して，脱髄と軸索傷害を増強する[5]．

現在欧米において，MS再発抑制のために，α4β1 integrin(VLA4)に対するヒト化モノクロナル抗体Natalizumabが臨床で用いられている．しかしながら，Natalizumabは進行性多巣性白質脳症(progressive multifocal leukoencephalopathy：PML)を惹起する危険性があり，より安全な薬の開発が必要である．分子ネットワークから創薬標的分子を探索する場合には，多数の分子からリレーションが集中しているハブ(hub)とよばれる中心分子を同定することが重要である．ハブの抑制薬または活性化薬は，ネットワークのロバストネスの維持に重大な影響を及ぼす．ECM-integrinシグナル伝達系は，炎症性脱髄遷延化の抑制薬の標的パスウェイであり，focal adhesion kinase(FAK)がハブとなる(**図1楕円**)．低分子化合物TAE226は，ECMによるFAKの自己リン酸化を選択的に抑制し，*in vivo*モデル系では経口投与により腫瘍細胞の増殖と血管新生を抑制する[6]．したがってTAE226はFAKを分子標的とするMS慢性炎症性脱髄抑制薬の候補となる可能性があり，EAEにおける前臨床試験の実施が待たれる．

3．Th17細胞分化関連遺伝子トランスクリプトーム解析からみた創薬標的分子

1990年代までMSは，IFN-γ投与で病態増悪を認めた過去の臨床試験の結果より，Th1病であるとみなされてきた．現在では，病態形成で中心的役割を果たしているのは，転写因子RAR-related orphan receptor C(RORC，RORγt)を発現し，IL-17A，IL-17F，IL-21，IL-22を産生するTh17細胞であるとの見解になった[7]．Th17細胞は，トランスフォーミング増殖因子(transforming growth factor：TGF)-βとIL-6，IL-21の存在下でナイーブT(Th0)細胞から分化誘導される．Th17細胞は，活動期RRMS患者の血液中では，非活動期や健常者に比較して7倍増加しており，これらの細胞は髄鞘抗原myelin basic protein(MBP)に対して反応性を示す[8]．Th17細胞は，MS脳では活動性病巣に集積している[9]．IFN-βは，Th1病には有効だがTh17病には無効であり，MSのIFN-βノンレスポンダーでは血清IL-17Fが増加している[10]．以上の所見をまとめると，Th17細胞分化制御関連遺伝子は，MSの創薬標的分子となり得る．

われわれは，公共の遺伝子発現データベースGene Expression Omnibus(GEO)に登録されているHuhらのトランスクリプトームデータセット(GSE27241)を再解析し，Th17細胞分化制御遺伝

子の分子ネットワークを同定した．彼らはRORγt欠損(knockout：KO)および野生型(wild-type：WT)C57BL/6マウスのリンパ節と脾臓から細胞自動解析-分離装置(fluorescence activated cell sorter：FACS)で分離した$CD4^+CD8^-CD19^-CD25^-CD44^{low/int}CD62L^+$ナイーブT細胞を，プレートコートした抗CD3ε抗体と抗CD28抗体で刺激し，さらにIL-6，TGF-β，抗IFN-γ抗体と抗IL-4抗体を添加した培地(Th17-inducing condition)で48時間培養して，Th17細胞の分化を誘導した[11]．また培養系にdimethyl sulfoxide(DMSO)またはDMSOに溶解したdigoxin(DIG：10 μM)を添加し，Th17細胞分化に対する抑制効果を調べた．GSE27241は，各条件の細胞からRNAを精製し，Mouse Genome 430 2.0 Array(Affymetrix)で解析し，robust multiarray average(RMA)法で正規化したデータセットである(WT-DMSO，WT-DIG，KO-DMSO，KO-DIG各2サンプル)．

われわれはHuhらのデータに関して，はじめにWT-DMSO群とKO-DMSO群を比較し，Th17-inducing conditionにおいて前者で2倍以上発現上昇した57遺伝子(Th17細胞分化関連遺伝子群)を同定した(**表1**)．つぎにWT-DIG群とWT-DMSO群を比較し，前者で0.5倍以下に発現低下した12遺伝子を同定した(DIG応答性遺伝子群)(**表1下線**)．また57遺伝子を指標として階層クラスター解析をおこなったところ，WT-DMSO，KO-DMSO，WT-DIG，KO-DIGの各群はおのおの独立したクラスターを形成し，WT-DIG群はKO-DMSO群に近接したクラスターに分類された(**図2**)．DIGで発現抑制された12遺伝子のうち11遺伝子は，ほかの遺伝子から独立したクラスターを形成し，11遺伝子を含む16遺伝子は転写が共調節(co-regulation)されている可能性がある(**図2点線**)．KeyMolnetの共通上流検索により，これらの16遺伝子に関連する分子ネットワークを解析したところ，TGF-β受容体シグナル伝達系で中心的な役割を果たしている転写因子SMADによる発現調節の関与が最も強く示唆された(p＝1.194E-060)(**図3**)．

TGF-β受容体の活性化に伴ってリン酸化されたSMAD2とSMAD3は，SMAD4と複合体を形成して核へ運ばれ，種々のコアクチベーターやコリプレッサーと協調して，標的遺伝子の転写を制御する．SMAD2はTh17細胞の分化に必須であると報告されている[12]．DIGは，Huhらが4812種類の低分子化合物に関して，RORγt転写活性化抑制を指標にスクリーニングし，RORγtと結合してTh17細胞の分化を抑制することが判明した化合物である[11]．またRORγt，RORαと結合してTh17細胞の分化を抑制する合成リガンドSR1001も報告されている[13]．DIGは転写因子SMADが制御している分子ネットワーク上のTh17細胞分化関連遺伝子群(**表1下線**)の発現を共抑制している可能性がある．SMAD系転写因子は分子ネットワークのハブに位置し，MSにおけるTh17細胞分化制御薬の標的分子と成りうる．しかしながら，TGF-β受容体シグナル系を全般的に抑制すると，induced $Foxp3^+$ regulatory T(iTreg)細胞の分化まで抑制してしまう可能性があること，SMAD非依存性のTh17細胞分化経路も存在すること[14]，SMAD2，SMAD3は機能的に冗長にはたらくこと，SMAD3それ自体はRORγtと結合してその活性を抑制し，Th17細胞の分化を負に制御していること[15]などを考慮し，SMAD系転写因子を選択的かつ部分的に抑制できるような新薬の開発が望ましい．

おわりに

膨大なオミックスデータに関与する分子ネットワークを手際よく解析するためには，精査された文献情報にもとづく解析ツールを使う必要がある．解析ツールはいまだ発展途上かつ日進月歩であり，現時点では，どのツールもスプライスバリアントや翻訳後修飾，細胞特異的発現，細胞内局在化，

表 1. Th17 細胞分化関連 57 遺伝子

Entrez Gene ID	Gene Symbol	Gene Name	Ratio
70337	iyd	iodotyrosine deiodinase	11.06
16171	IL17A	interleukin 17A	4.30
76142	ppp1r14c	protein phosphatase 1, regulatory(inhibitor)subunit 14c	4.25
193740	Hspa1a	heat shock protein 1A	3.47
50929	il22	interleukin 22	3.39
15511	Hspa1b	heat shock protein 1B	3.38
56312	nupr1	nuclear protein 1	3.23
14538	GCNT2	glucosaminyl(N-acetyl)transferase 2, I-branching enzyme	2.79
74103	Nebl	nebulette	2.76
75573	2310007L24Rik	RIKEN cDNA 2310007L24 gene	2.55
68549	SGOL2	shugoshin-like 2(S. pombe)	2.53
237436	GAS2L3	growth arrest-specific 2 like 3	2.47
76131	depdc1a	DEP domain containing 1a	2.43
100043766	Gm14057	predicted gene 14057	2.37
14235	FOXM1	forkhead box M1	2.37
230098	E130306D19Rik	RIKEN cDNA E130306D19 gene	2.30
171284	Timd2	T-cell immunoglobulin and mucin domain containing 2	2.29
12235	BUB1	budding uninhibited by benzimidazoles 1 homolog(S. cerevisiae)	2.26
51944	D2Ertd750e	DNA segment, Chr 2, ERATO Doi 750, expressed	2.24
17863	myb	myeloblastosis oncogene	2.24
229841	CENPE	centromere protein E	2.22
270906	PRR11	proline rich 11	2.19
12316	ASPM	asp(abnormal spindle)-like, microcephaly associated(Drosophila)	2.18
108000	CENPF	centromere protein F	2.18
17345	MKI67	antigen identified by monoclonal antibody Ki 67	2.16
14432	gap43	growth associated protein 43	2.15
105988	ESPL1	extra spindle poles-like 1(S. cerevisiae)	2.15
15366	HMMR	hyaluronan mediated motility receptor(RHAMM)	2.15
27053	asnS	asparagine synthetase	2.15
52276	CDCA8	cell division cycle associated 8	2.15
18005	NEK2	NIMA(never in mitosis gene a)-related expressed kinase 2	2.15
72080	2010317E24Rik	RIKEN cDNA 2010317E24 gene	2.15
74107	CEP55	centrosomal protein 55	2.13
29817	igfbp7	insulin-like growth factor binding protein 7	2.13
71819	KIF23	kinesin family member 23	2.10
75317	4930547N16Rik	RIKEN cDNA 4930547N16 gene	2.10
12704	CIT	citron	2.10
72140	CCDC123	coiled-coil domain containing 123	2.08
234258	Neil3	nei like 3(E. coli)	2.08
12442	CCNB2	cyclin B2	2.07
72119	Tpx2	TPX2, microtubule-associated protein homolog(Xenopus laevis)	2.07
68743	Anln	anillin, actin binding protein	2.06
20419	SHCBP1	Shc SH2-domain binding protein 1	2.05
208084	PIF1	PIF1 5'-to-3'DNA helicase homolog(S. cerevisiae)	2.04
17279	Melk	maternal embryonic leucine zipper kinase	2.04
19348	kif20a	kinesin family member 20A	2.04
21335	TACC3	transforming, acidic coiled-coil containing protein 3	2.03
208628	KNTC1	kinetochore associated 1	2.02
19659	Rbp1	retinol binding protein 1, cellular	2.02
72155	CENPN	centromere protein N	2.02
257630	Il17f	interleukin 17F	2.02
215819	nhsl1	NHS-like 1	2.02
54141	SPAG5	sperm associated antigen 5	2.01
12189	BRCA1	breast cancer 1	2.01
19362	RAD51AP1	RAD51 associated protein 1	2.01
110033	Kif22	kinesin family member 22	2.00
69534	AVPI1	arginine vasopressin-induced 1	2.00

GSE27241 は RORγt 欠損(knockout：KO)および野生型(wild-type：WT)マウスナイーブ T 細胞を，Th17-inducing condition で 48 時間培養して Th17 細胞の分化を誘導し，培養系に DMSO に溶解した digoxin(DIG)を添加した細胞のトランクリプトームデータである．GSE27241 に関して，はじめに WT-DMSO と KO-DMSO を比較し，Th17-inducing condition において前者で 2 倍以上発現上昇した Th17 細胞分化関連 57 遺伝子を同定した．つぎに WT-DIG と WT-DMSO を比較し，前者で 0.5 倍以下に発現低下した DIG 応答性 12 遺伝子を同定した(下線)．

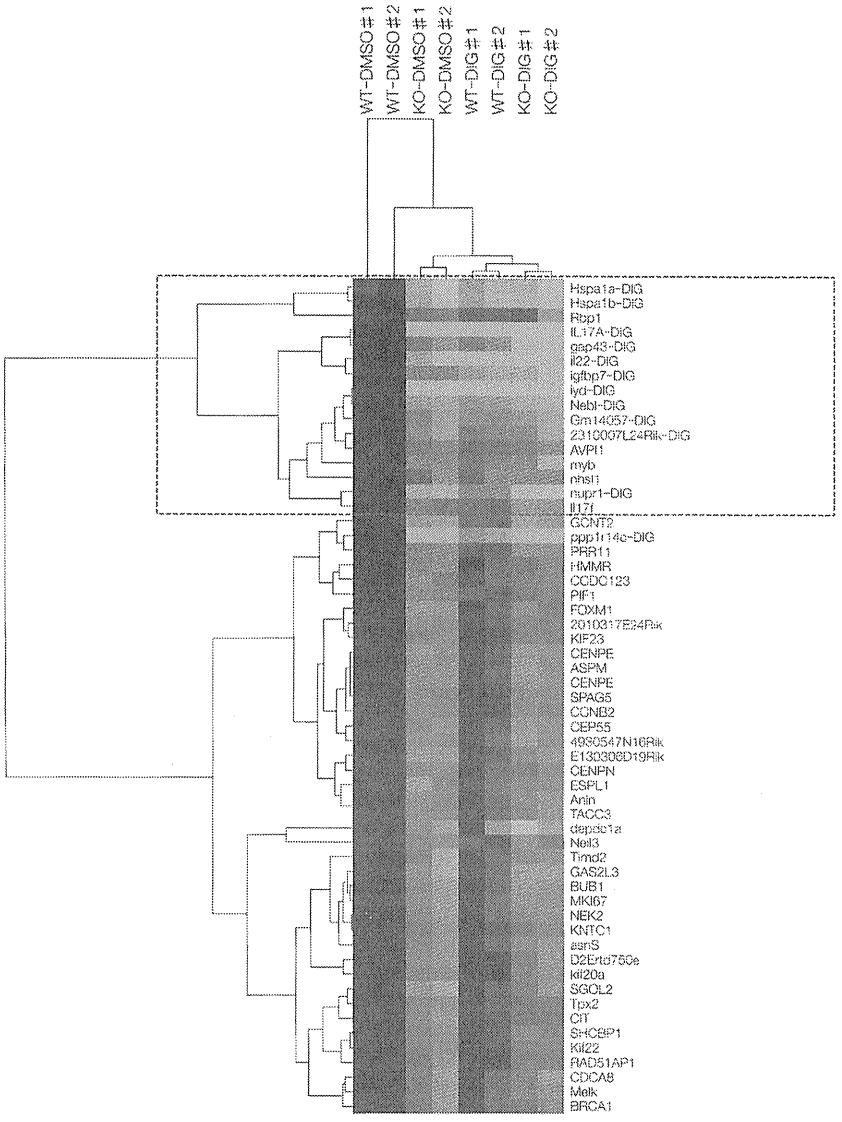

図 2. Th17 細胞分化関連 57 遺伝子の階層クラスター解析

GSE27241 は，RORγt 欠損(knockout：KO)および野生型(wild-type：WT)マウスナイーブ T 細胞を，Th17-inducing condition で 48 時間培養し，Th17 細胞の分化を誘導．培養系に DMSO に溶解した digoxin(DIG)を添加した細胞のトランクリプトームデータである．はじめに WT-DMSO と KO-DMSO を比較し，Th17 細胞分化関連 57 遺伝子を同定し，階層クラスター解析をおこなった．つぎに WT-DIG と WT-DMSO を比較し，DIG 応答性 12 遺伝子を同定した(図の遺伝子-DIG)．DIG 応答性 11 遺伝子は独立したクラスターを形成し，これらを含む 16 遺伝子は転写が共調節(co-regulation)されている可能性がある(点線)．

動的な特性に関しては十分対応できていない．しかしながら生命現象を複雑なシステムとして捉えるシステム生物学的観点からすると，分子ネットワークを詳細に解析することにより，はじめて論理的な仮説に裏づけられた創薬標的分子を効率的に同定することができる．

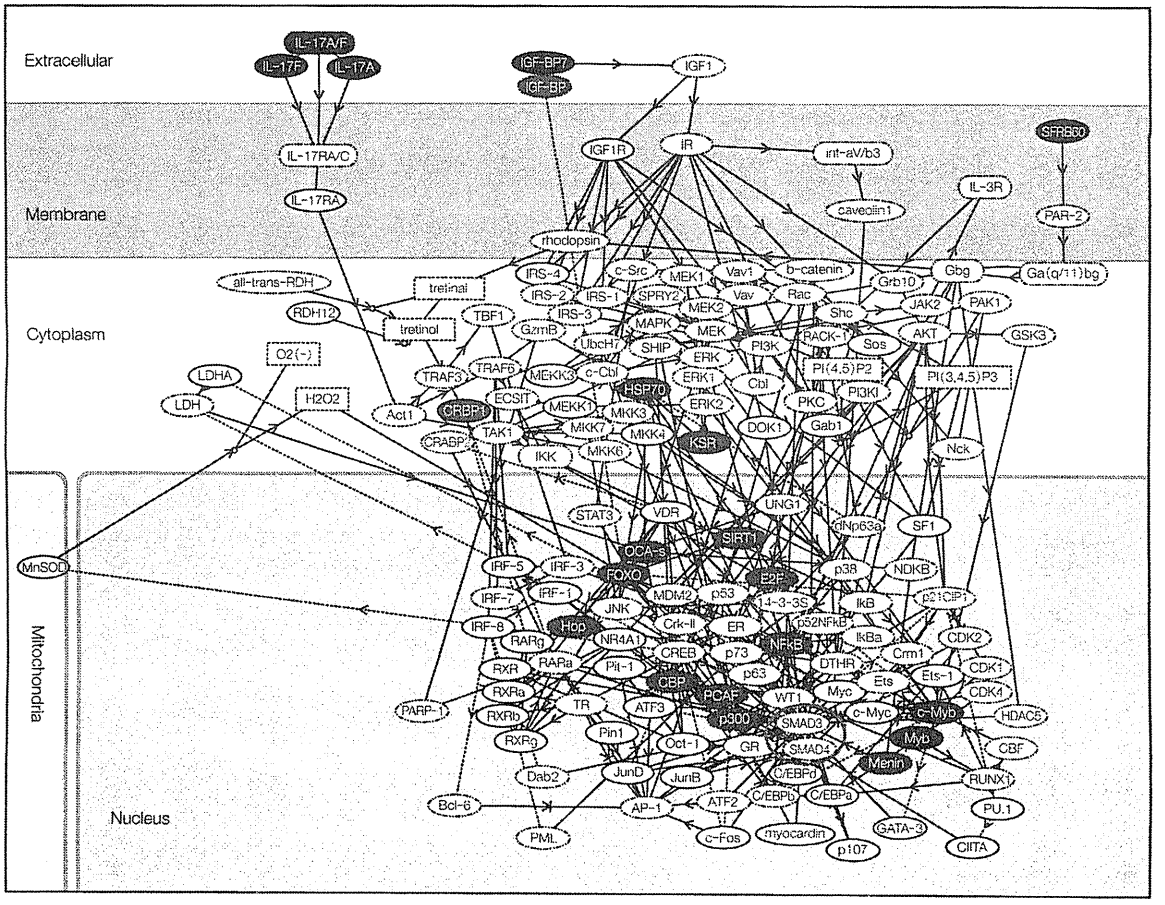

図 3. DIG 応答性 Th17 細胞分化関連遺伝子の分子ネットワーク解析
KeyMolnet 共通上流検索(コアコンテンツ：発現制御・直接結合・複合体形成)により，DIG 応答性 11 遺伝子のクラスターの 16 遺伝子(図 2)に関連する分子ネットワークを解析した．転写因子 SMAD(楕円)による発現調節の関与が示唆された．

謝辞

本稿で紹介した研究は，国立精神・神経医療研究センター神経研究所免疫研究部 山村隆部長，明治薬科大学バイオインフォマティクス 天竺桂弘子助教との共同研究でなされ，文部科学省基盤研究(C22500322)と私立大学戦略的研究基盤形成支援事業明治薬科大学ハイテクリサーチセンター研究事業(S0801043)および厚生労働科学難治性疾患克服研究事業(H21-難治-一般-201：H22-難治-一般-136)の補助を受けた．

文 献

1) Satoh J：Bioinformatics approach to identifying molecular biomarkers and networks in multiple sclerosis. *Clin Exp Neuroimmunol* **1**：127-140, 2010
2) Han MH *et al*：Proteomic analysis of active multiple sclerosis lesions reveals therapeutic targets. *Nature* **451**：1076-1081, 2008
3) Satoh JI *et al*：Molecular network of the comprehensive multiple sclerosis brain-lesion proteome. *Mult Scler* **15**：531-541, 2009
4) van Horssen J *et al*：The extracellular matrix in multiple sclerosis pathology. *J Neurochem* **103**：1293-1301, 2007
5) Milner R *et al*：Fibronectin- and vitronectin-induced microglial activation and matrix metallo-

proteinase-9 expression is mediated by integrins $\alpha_5\beta_1$ and $\alpha_v\beta_5$. *J Immunol* **178** : 8158-8167, 2007
6) Liu TJ *et al* : Inhibition of both focal adhesion kinase and insulin-like growth factor-I receptor kinase suppresses glioma proliferation in vitro and in vivo. *Mol Cancer Ther* **6** : 1357-1367, 2007
7) McFarland HF *et al* : Multiple sclerosis : a complicated picture of autoimmunity. *Nat Immunol* **8** : 913-919, 2007
8) Durelli L *et al* : T-helper 17 cells expand in multiple sclerosis and are inhibited by interferon-β. *Ann Neurol* **65** : 499-509, 2009
9) Tzartos JS *et al* : Interleukin-17 production in central nervous system-infiltrating T cells and glial cells is associated with active disease in multiple sclerosis. *Am J Pathol* **172** : 146-155, 2008
10) Axtell RC *et al* : T helper type 1 and 17 cells determine efficacy of interferon-β in multiple sclerosis and experimental encephalomyelitis. *Nat Med* **16** : 406-412, 2010
11) Huh JR *et al* : Digoxin and its derivatives suppress T_H17 cell differentiation by antagonizing RORγt activity. *Nature* **472** : 486-490, 2011
12) Malhotra N *et al* : SMAD2 is essential for TGFβ-mediated Th17 cell generation. *J Biol Chem* **285** : 29044-29048, 2010
13) Solt LA *et al* : Suppression of T_H17 differentiation and autoimmunity by a synthetic ROR ligand. *Nature* **472** : 491-494, 2011
14) Lu L *et al* : Role of SMAD and non-SMAD signals in the development of Th17 and regulatory T cells. *J Immunol* **184** : 4295-4306, 2010
15) Martinez GJ *et al* : Smad3 differentially regulates the induction of regulatory and inflammatory T cell differentiation. *J Biol Chem* **284** : 35283-35286, 2009

Influenza infection in suckling mice expands an NKT cell subset that protects against airway hyperreactivity

Ya-Jen Chang,[1] Hye Young Kim,[1] Lee A. Albacker,[1] Hyun Hee Lee,[1] Nicole Baumgarth,[2] Shizuo Akira,[3] Paul B. Savage,[4] Shin Endo,[5] Takashi Yamamura,[6] Janneke Maaskant,[7] Naoki Kitano,[8] Abel Singh,[9] Apoorva Bhatt,[9] Gurdyal S. Besra,[9] Peter van den Elzen,[8] Ben Appelmelk,[7] Richard W. Franck,[10] Guangwu Chen,[10] Rosemarie H. DeKruyff,[1] Michio Shimamura,[5,6,11] Petr Illarionov,[9] and Dale T. Umetsu[1]

[1]Division of Immunology and Allergy, Children's Hospital, Harvard Medical School, Boston, Massachusetts, USA. [2]Center for Comparative Medicine, University of California, Davis, California, USA. [3]WPI Immunology Frontier Research Center, Osaka University, Osaka, Japan. [4]Brigham Young University, Provo, Utah, USA. [5]Mitsubishi Kagaku Institute of Life Sciences, Tokyo, Japan. [6]National Center of Neurology and Psychiatry, Tokyo, Japan. [7]Department of Medical Microbiology, Vrje University Medical Center, Amsterdam, the Netherlands. [8]Child and Family Research Institute, University of British Columbia, Vancouver, Canada. [9]University of Birmingham, School of Biosciences, Birmingham, United Kingdom. [10]Hunter College of CUNY, New York, New York, USA. [11]University of Tsukuba, Ibaraki, Japan.

Infection with influenza A virus represents a major public health threat worldwide, particularly in patients with asthma. However, immunity induced by influenza A virus may have beneficial effects, particularly in young children, that might protect against the later development of asthma, as suggested by the hygiene hypothesis. Herein, we show that infection of suckling mice with influenza A virus protected the mice as adults against allergen-induced airway hyperreactivity (AHR), a cardinal feature of asthma. The protective effect was associated with the preferential expansion of $CD4^-CD8^-$, but not $CD4^+$, NKT cells and required T-bet and TLR7. Adoptive transfer of this cell population into allergen-sensitized adult mice suppressed the development of allergen-induced AHR, an effect associated with expansion of the allergen-specific forkhead box $p3^+$ ($Foxp3^+$) Treg cell population. Influenza-induced protection was mimicked by treating suckling mice with a glycolipid derived from *Helicobacter pylori* (a bacterium associated with protection against asthma) that activated NKT cells in a CD1d-restricted fashion. These findings suggest what we believe to be a novel pathway that can regulate AHR, and a new therapeutic strategy (treatment with glycolipid activators of this NKT cell population) for asthma.

Introduction

Bronchial asthma, a complex and heterogeneous trait, is a major public health problem, affecting nearly 10% of the general population and disproportionately affecting children. Moreover, the prevalence of asthma has increased dramatically over the past 3 decades, an increase thought to be due to changes in our environment. These environmental changes include reductions in the incidence of infectious diseases that may exert protective effects against asthma, as suggested by the hygiene hypothesis (1). While the infectious agents responsible for this relationship, and the precise mechanisms by which infectious microorganisms might protect against asthma, are very poorly understood, epidemiological studies suggest that infection with bacteria (e.g., *Helicobacter pylori* [refs. 2, 3], endotoxin [ref. 4], or *Acinetobacter lwoffii* [ref. 5]) or viruses (e.g., hepatitis A virus [refs. 6, 7]) might reduce the likelihood of developing asthma.

The role of viral infection in modulating the development of asthma is particularly complex because many different viruses affect the respiratory tract, some appearing to enhance and some to protect against the development of asthma. For example, infection with human rhinovirus in children before 3 years of age increases the later risk of developing asthma (8), while other respiratory viral infections appear to protect against the later development of asthma (9–14). However, in older individuals with established asthma, respiratory viral infection, particularly with influenza A virus, almost always triggers acute symptoms of asthma (15–17). These discrepancies may be due to the timing of the infection, since infection in very young children may profoundly alter the developing innate immune system in such a way as to protect against the later development of asthma, or to the specific immunological cell types activated by a given infectious agent.

To improve our understanding of the role of respiratory viral infection in children in the development of asthma, we studied a mouse model of asthma in which suckling mice were infected with the influenza A virus (H3N1), and were subsequently studied as adults for susceptibility to allergen-induced airway hyperreactivity (AHR), a cardinal feature of asthma. We found that H3N1 infection in suckling mice protected the mice as adults against allergen-induced AHR. The protective effect was associated with the preferential expansion of a subpopulation of suppressive double-negative (DN) NKT cells and was mimicked by treatment of suckling mice with several specific glycolipids, including one derived from *H. pylori*.

Results

Infection of suckling mice with H3N1 protects against AHR. We infected suckling pups (2 weeks old) or adult mice (8 weeks old) with the influenza A/Mem71 (H3N1) virus, and 6 weeks later the mice were examined for susceptibility to OVA-induced AHR (Figure 1A). H3N1 infection

Authorship note: Michio Shimamura, Petr Illarionov, and Dale T. Umetsu contributed equally to this work.

Conflict of interest: The authors have declared that no conflict of interest exists.

Citation for this article: *J Clin Invest.* 2011;121(1):57–69. doi:10.1172/JCI44845.

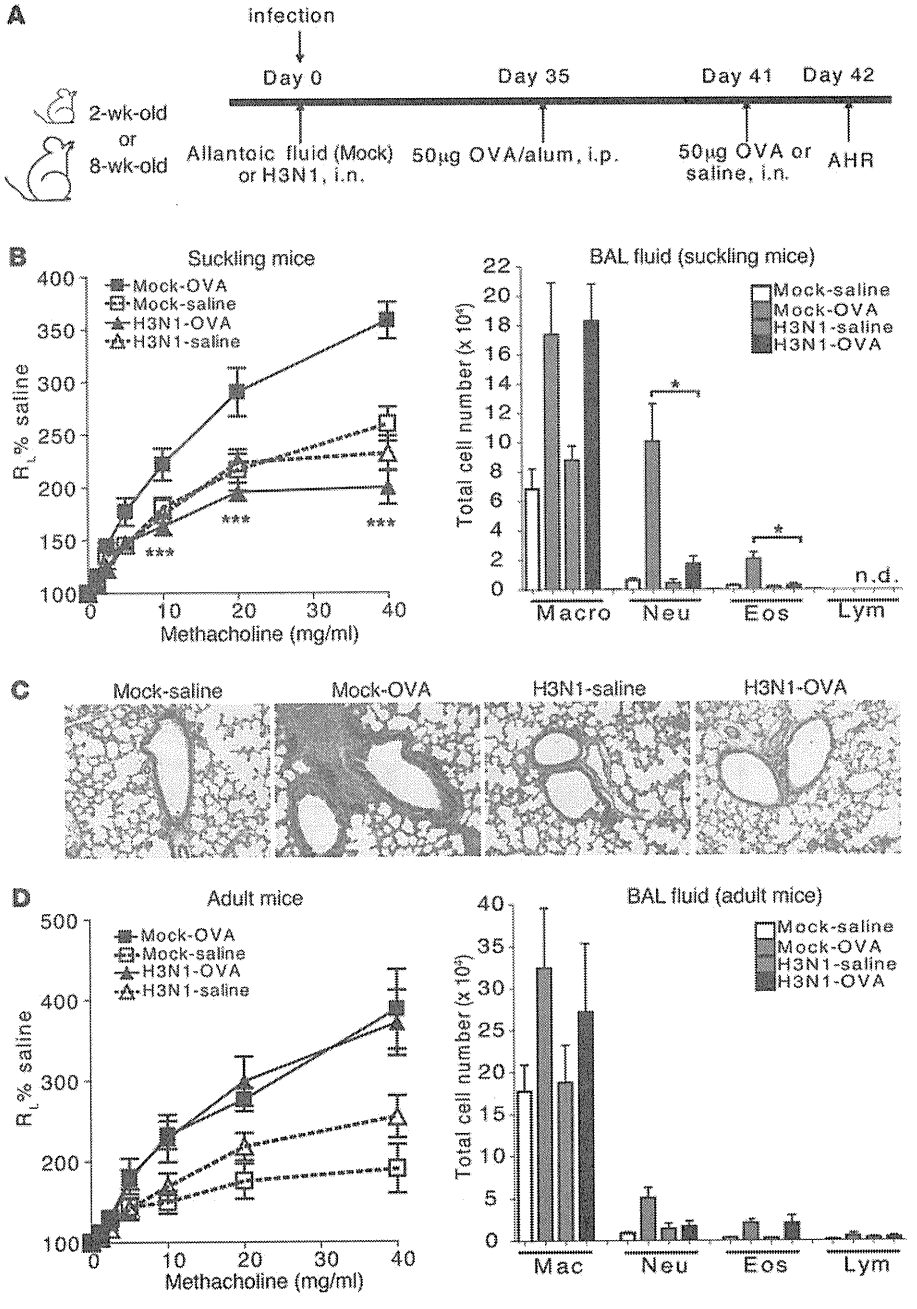

Figure 1
Infection of suckling mice with H3N1 protects the mice against AHR when adults. (**A**) Schematic showing the protocol for OVA-induced AHR. Two-week-old (suckling) or 8 week-old (adult) mice were treated with influenza A virus (H3N1) or control AF (mock infection) and assessed 6 weeks later as adults for AHR. (**B**) BALB/c mice ($n = 8$ per group) treated with H3N1 or AF at 2 weeks of age were assessed 42 days after infection for OVA-induced AHR. Changes in lung resistance (R_L) were measured in anesthetized, tracheotomized, intubated, and mechanically ventilated mice (left panel). ***$P < 0.001$ compared with mock-infected group. Cells in BAL were collected and analyzed 24 hours after the final OVA challenge (right panel). *$P < 0.05$ compared with mock-infected group. (**C**) Representative lung sections stained with H&E (original magnification, ×10) from mock- or H3N1-infected mice treated with saline or challenged with OVA. (**D**) Eight-week-old BALB/c mice ($n = 5$ per group) were infected with H3N1 or AF. Six weeks after infection, the mice were assessed for OVA-induced AHR by measuring lung resistance (left panel). Cells in BAL were collected and analyzed 24 hours after the final OVA challenge (right panel). Data are representative of 3 independent experiments.

in 2-week-old mice protected the mice as adults (at 8 weeks of age) against OVA-induced AHR (Figure 1B) and airway inflammation (Figure 1, B and C). In contrast, severe OVA-induced AHR and airway inflammation developed in the mock-infected mice at 8 weeks of age. Whereas infection in 2-week-old suckling mice conferred protection, infection in 8-week-old adult mice with H3N1 did not protect against subsequent OVA-induced AHR or airway inflammation (Figure 1D).

Adoptive transfer of NKT cells cannot reconstitute OVA-induced AHR in Jα18$^{-/-}$ mice. Infection with a different influenza virus strain (H3N2) enhanced the ability of respiratory tolerance to prevent OVA-induced AHR (11), consistent with the idea that influenza infection is complex and can affect multiple compartments of the immune system. Because infection with the influenza A virus has been shown to directly activate NKT cells (18), which play a very important role in asthma (19), we asked whether infection with the H3N1 virus affected the function of NKT cells. We therefore purified NKT cells from mice infected with H3N1 as sucklings (42 days after infection) and adoptively transferred these cells (92%–97% purity; Supplemental Figure 1A; supplemental material available online with this article; doi:10.1172/JCI44845DS1) into adult OVA-sensitized, NKT cell–deficient recipients (Jα18$^{-/-}$ mice) (Figure 2A). After receiving the H3N1-exposed NKT cells, the Jα18$^{-/-}$ mice, which have CD1d-restricted non-invariant (but not invariant) TCR NKT cells, and which cannot develop

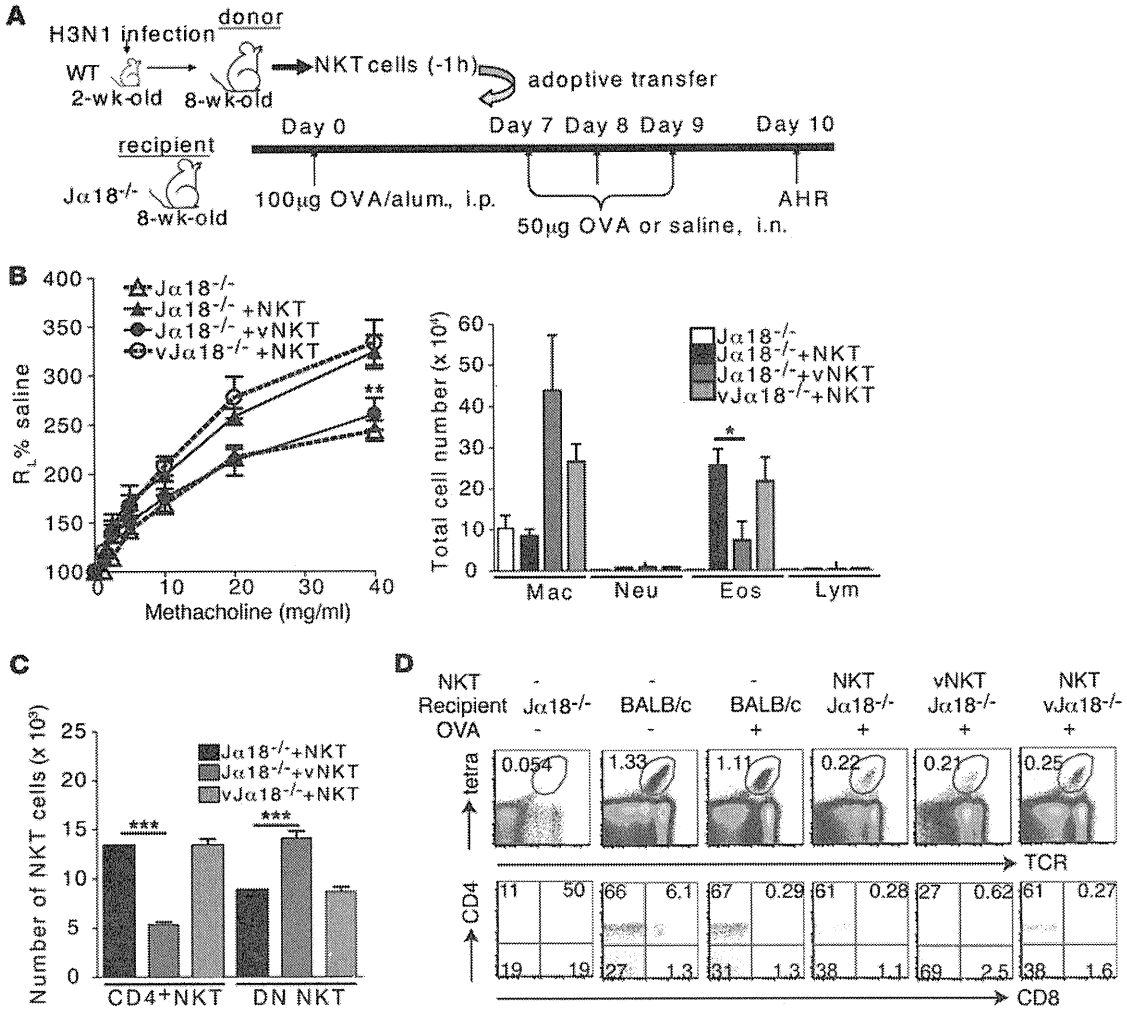

Figure 2

Adoptive transfer of H3N1-exposed NKT cells fails to reconstitute OVA-induced AHR. (**A**) Schematic showing the protocol for adoptive transfer of NKT cells to OVA-immunized *Jα18*$^{-/-}$ recipients. The donor mice were infected with H3N1 or mock infected at 2 weeks of age. Six weeks after infection, NKT cells were purified and adoptively transferred into OVA-sensitized *Jα18*$^{-/-}$ mice, which were then challenged with OVA and assessed for AHR. (**B**) Adoptive transfer of H3N1-exposed NKT cells (vNKT) to *Jα18*$^{-/-}$ mice failed to reconstitute OVA-induced AHR (measured as lung resistance in response to methacholine challenge) (left panel). Adoptive transfer of NKT cells from mock-infected mice (NKT) fully reconstituted AHR. H3N1 infection at 2 weeks of age of *Jα18*$^{-/-}$ mice (*vJα18*$^{-/-}$) and reconstitution at 8 weeks of age with NKT cells from mock-infected mice did not protect against AHR (n = 8–10 per group). BAL fluid was collected and analyzed (right panel). $^{*}P < 0.05$ and $^{**}P < 0.01$, compared with *Jα18*$^{-/-}$ + NKT group. (**C** and **D**) Lung cells were isolated from the recipients after measurement of AHR, and the absolute numbers (**C**) and percentages (**D**) of lung CD4^{+} or CD4^{-}CD8^{-} (DN) NKT subsets were assessed by FACS. Upper panels show dot plots for NKT cells in lung leukocytes. After gating on the NKT cells, the cells were analyzed for CD4 and CD8 (lower panels). $^{***}P < 0.001$ compared with WT NKT group. Data are representative of 3 independent experiments.

allergen-induced AHR unless reconstituted with functional invariant TCR NKT cells (20–22), failed to develop OVA-induced AHR (Figure 2B). In contrast, transfer of NKT cells from mock-infected mice to *Jα18*$^{-/-}$ mice fully reconstituted AHR. Moreover, H3N1 infection in 2-week-old *Jα18*$^{-/-}$ suckling mice (*vJα18*$^{-/-}$ mice) and later reconstitution (at 8 weeks of age) with NKT cells from mock-infected mice did not prevent OVA-induced AHR (Figure 2B), indicating that early exposure of all of the non-NKT cells in *Jα18*$^{-/-}$ mice (e.g., conventional CD4^{+} and CD8^{+} T cells) to H3N1 was not effective in preventing AHR. Finally, in the lungs of mice receiving the H3N1 virus–exposed NKT cells (42 days after infection), significantly more CD4^{-}CD8^{-} (DN) NKT cells and significantly fewer CD4^{+} NKT cells were present (Figure 2, C and D), suggesting that H3N1 infection of 2-week-old suckling mice reduced the inflammatory function of the NKT cells, possibly by altering the CD4^{+} versus DN NKT cell subset proportions.

H3N1 infection accelerates the expansion of pulmonary NKT cells in suckling mice. In 2-week-old naive suckling mice, few NKT cells were present in the lungs, although this number increased normally to adult levels over a 6-week period (Figure 3A). Importantly, H3N1 infection but not mock infection in suckling mice greatly accelerated the expansion of the pulmonary NKT cell numbers (Figure 3B).

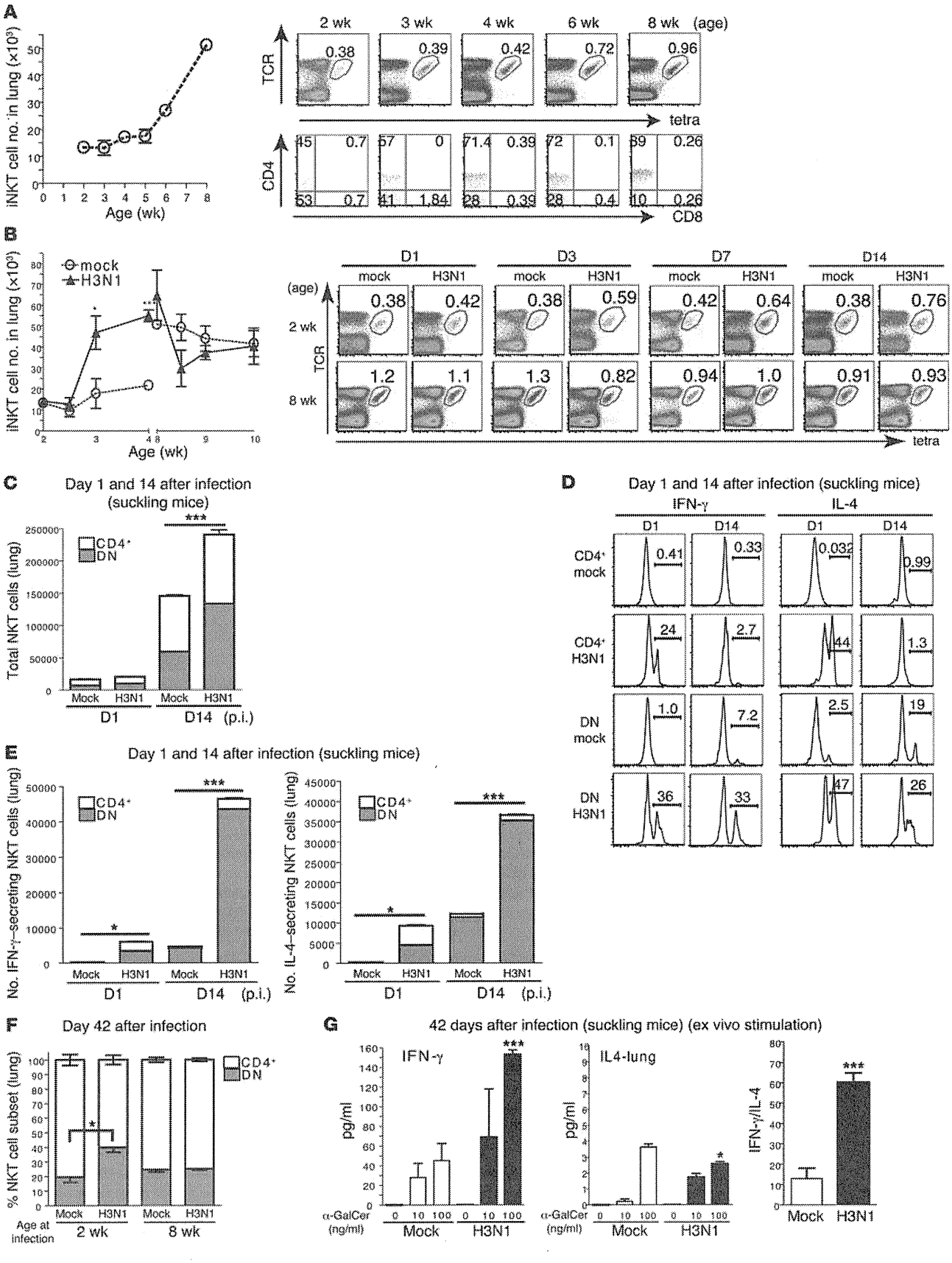
A
iNKT cell no. in lung (×10³)
Age (wk)
2 wk
3 wk
4 wk
6 wk
8 wk (age)
TCR
tetra
CD4
CD8
0.38
0.39
0.42
0.72
0.96
B
mock
H3N1
D1
D3
D7
D14
(age)
2 wk
8 wk
0.38
0.42
0.38
0.59
0.42
0.64
0.38
0.76
1.2
1.1
1.3
0.82
0.94
1.0
0.91
0.93
C
Day 1 and 14 after infection (suckling mice)
Total NKT cells (lung)
CD4⁺
DN
Mock
H3N1
D1
D14 (p.i.)
D
Day 1 and 14 after infection (suckling mice)
IFN-γ
IL-4
CD4⁺ mock
CD4⁺ H3N1
DN mock
DN H3N1
0.41
0.33
0.032
0.99
24
2.7
44
1.3
1.0
7.2
2.5
19
36
33
47
26
E
Day 1 and 14 after infection (suckling mice)
No. IFN-γ–secreting NKT cells (lung)
No. IL-4–secreting NKT cells (lung)
F
Day 42 after infection
% NKT cell subset (lung)
Age at infection
2 wk
8 wk
G
42 days after infection (suckling mice) (ex vivo stimulation)
IFN-γ
IL4-lung
IFN-γ/IL-4
pg/ml
α-GalCer (ng/ml)
0
10
100
Mock
H3N1

Figure 3
H3N1 infection in 2-week-old mice alters the phenotype of the NKT cells. (**A**) Lung cells were isolated over a 6-week period and analyzed for NKT cells. Left: Absolute numbers of lung NKT cells. Right: Percentage of NKTs (top) in lung leukocytes. NKT cells were analyzed for CD4 and CD8 (bottom). (**B**) Left: BALB/c mice (n = 3/group) were infected with H3N1 or AF at 2 or 8 weeks of age, and lung NKT cells were assessed over 2 weeks. Right: Percentage of NKT cells in lungs of 2-week-old and 8-week-old mice. (**C**) Two-week-old BALB/c mice were mock infected or infected with H3N1, and pulmonary CD4$^+$ NKT and DN NKT cell numbers were assessed on days 1 and 14 after infection. (**D** and **E**) NKT cells from **C** were assessed for CD4, IFN-γ, and IL-4 expression (**D**) and absolute numbers quantified (**E**). (**F**) BALB/c mice (n = 4–5/group) were infected with H3N1 or mock infected at 2 or 8 weeks of age, and lung samples were taken 42 days later to assess NKT cell subsets. One of 2 independent experiments is shown. (**G**) Two-week-old BALB/c mice were infected with H3N1 or mock infected. After 42 days, lung cells were harvested and stimulated ex vivo with vehicle or α-GalCer for 96 hours. IFN-γ and IL-4 in supernatants from triplicate wells were determined by ELISA and the IFN-γ/IL-4 ratio calculated. $^*P < 0.05$, $^{***}P < 0.001$ compared with mock infection.

In contrast, H3N1 infection in adult mice had little effect on pulmonary NKT cell numbers. In fact, H3N1 infection in the adult mice transiently reduced the number of NKT cells, possibly due to activation-induced TCR downregulation (Figure 3B). In 2-week-old suckling naive mice, approximately 50% of the pulmonary NKT cells were CD4$^+$, and over time this fraction increased such that in 8-week-old adult naive mice, 89% of the pulmonary NKT cells were CD4$^+$ (dot plots in Figure 3A). However, H3N1 infection of suckling mice preferentially increased the number of DN NKT cells by day 14 after infection (Figure 3C). Both CD4$^+$ and DN NKT cells from the suckling mice secreted IFN-γ on day 1 of infection, but 14 days after infection only DN but not CD4$^+$ pulmonary NKT cells continued to secrete IFN-γ (and IL-4), as assessed with intracellular staining without in vitro restimulation (Figure 3D). Thus, 14 days after infection the great majority of cytokine-secreting cells in the lungs were DN NKT cells (Figure 3E).

Analysis of the mice 42 days after H3N1 infection showed that the proportion of DN versus CD4$^+$ NKT cells in the lungs doubled, whereas 42 days after H3N1 infection in 8-week-old mice, there was no effect on the proportion of DN NKT cells in the lungs (Figure 3F). Assessment of the cytokine profile of NKT cells 42 days following infection after ex vivo stimulation with α-galactosylceramide (α-GalCer, which specifically activates NKT cells) demonstrated increased IFN-γ but not IL-4 production by the H3N1-exposed NKT cells (Figure 3G), resulting in a greatly increased IFN-γ/IL-4 ratio (Figure 3G). These results suggested that H3N1 infection in suckling mice preferentially expanded a unique NKT cell population in the lungs that, by day 42, preferentially produced IFN-γ but not IL-4 and was associated with a reduced expression of CD4.

Adoptive transfer of H3N1-exposed NKT cells suppresses AHR and induces Treg cells. While the H3N1-exposed NKT cells (vNKT) could not induce AHR when transferred into *Jα18*$^{-/-}$ mice (Figure 2), they were not anergic, but instead potently suppressed OVA-induced AHR (Figure 4, A and B) and inflammation (Figure 4C), as assessed by adoptive transfer 42 days after infection into adult WT OVA-sensitized mice. In contrast, NKT cells from mock-infected mice (WT NKT) (Figure 4, B and C) or from adult mice infected with H3N1 (data not shown) did not suppress OVA-induced AHR. The proportion of DN NKT cells in the lungs of mice receiving the H3N1 virus–exposed NKT cells was increased (Figure 4D), consistent with the idea that H3N1 infection in suckling mice preferentially expands a subpopulation of DN NKT cells.

To more clearly demonstrate that the DN NKT cell subpopulation was responsible for the suppression of AHR, we purified CD4$^+$ and DN NKT cell subpopulations from the spleens of mice (purity 96%–99%) (Supplemental Figure 1C), which had been infected with H3N1, and adoptively transferred these cells into OVA-sensitized mice. Figure 4E shows that the DN but not the CD4$^+$ NKT cell population suppressed AHR that developed on challenge of the mice with OVA, confirming that the H3N1-exposed DN NKT cell population was responsible for this effect.

The suppression of AHR by the transferred H3N1-exposed NKT cells was associated with a 50% increase in the number of natural Foxp3$^+$ Treg cells and with a 300% increase in the number of adaptive OVA-specific Foxp3$^+$ Treg cells in the lungs (assessed by transferring DO11.10 Tg OVA-specific Foxp3$^-$ T cells from DO11.10 Tg × *Rag*$^{-/-}$ mice), compared with when NKT cells from mock-infected mice were transferred (Figure 4F). Furthermore, the inhibitory effect of the NKT cells exposed to H3N1 was reversed by treatment of the recipient mice with an anti-CD25 mAb (Figure 4G). These results together indicated that H3N1-exposed NKT cells could suppress the development of experimental asthma, and that natural and adaptive Treg cells might mediate the suppressive effects of the NKT cell population.

We found a similar suppressive NKT cell population in Vα14 TCR Tg mice. Adult Vα14 TCR transgenic mice have a 5- to 10-fold increase in the number of NKT cells in the spleen, of which the majority (53%) are DN NKT cells (Supplemental Figure 1B), whereas in WT BALB/c mice, only 11% of the splenic NKT cells are DN (Supplemental Figure 1B). Adoptive transfer of NKT cells purified from Vα14 TCR Tg mice into adult WT OVA-sensitized BALB/c mice greatly suppressed the development of OVA-induced AHR and airway inflammation (Figure 4, H–J). Transfer of Vα14 TCR Tg NKT cells was also associated with a 50% increase in the number of natural Foxp3$^+$ Treg cells and in a 300% increase in the number of adaptive OVA-specific Foxp3$^+$ Treg cells (assessed by transfer of DO11.10 Tg OVA-specific cells), compared with transfer of naive (WT) NKT cells (Figure 4F). These results suggest that NKT cells in Vα14 Tg mice were similar to NKT cells from suckling mice exposed to H3N1, in that they had suppressive activity for allergen-induced AHR.

The protective effect of H3N1 infection depends on TLR7 and T-bet. Since influenza A virus is a single-stranded RNA (ssRNA) virus, and since T-bet participates in IFN-γ production and in NKT cell maturation (23), we infected 2-week-old *Tlr7*$^{-/-}$*Tbet*$^{-/-}$ mice and control WT BALB/c mice with the H3N1 virus. Six weeks later, the mice were examined for OVA-induced AHR (protocol shown in Figure 5A). Whereas H3N1 infection in suckling WT mice protected against subsequent OVA-induced AHR and airway inflammation (Figure 5, B and C), H3N1 infection in suckling *Tlr7*$^{-/-}$ or suckling *Tbet*$^{-/-}$ mice failed to protect against, and even exacerbated, OVA-induced AHR and airway inflammation. Furthermore, the ratio of IFN-γ production to IL-4 production in NKT cells from *Tlr7*$^{-/-}$ mice was reduced (Supplemental Figure 2D), while IFN-γ was reduced and IL-13 and IL-17 production increased in NKT cells in *Tbet*$^{-/-}$ mice compared with WT mice (Supplemental Figure 2, A and E). (Note that *Tbet*$^{-/-}$ mice have reduced numbers of NKT cells, particularly in the liver [ref. 23] but have significant numbers of pulmonary NKT cells compared with WT mice [ref. 24]).

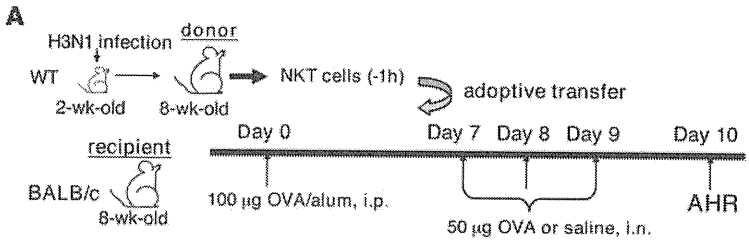
A
H3N1 infection
donor
WT
2-wk-old
8-wk-old
NKT cells (-1h)
adoptive transfer
recipient
BALB/c
8-wk-old
Day 0
Day 7
Day 8
Day 9
Day 10
100 μg OVA/alum, i.p.
50 μg OVA or saline, i.n.
AHR

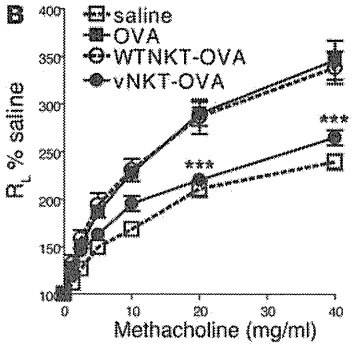
B
saline
OVA
WTNKT-OVA
vNKT-OVA
R_L % saline
Methacholine (mg/ml)

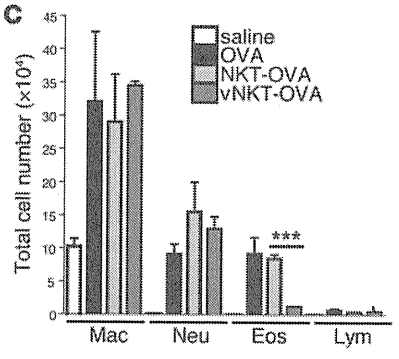
C
saline
OVA
NKT-OVA
vNKT-OVA
Total cell number (×10⁴)
Mac
Neu
Eos
Lym

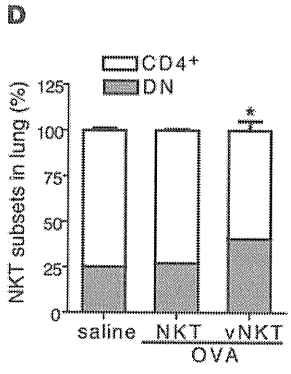
D
CD4+
DN
NKT subsets in lung (%)
saline
NKT
vNKT
OVA

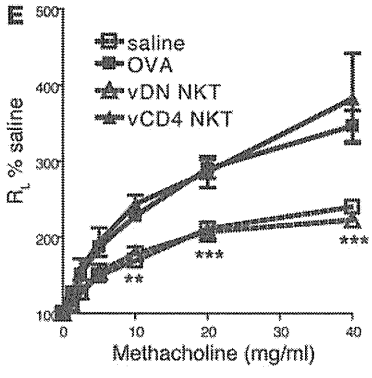
E
saline
OVA
vDN NKT
vCD4 NKT
R_L % saline
Methacholine (mg/ml)

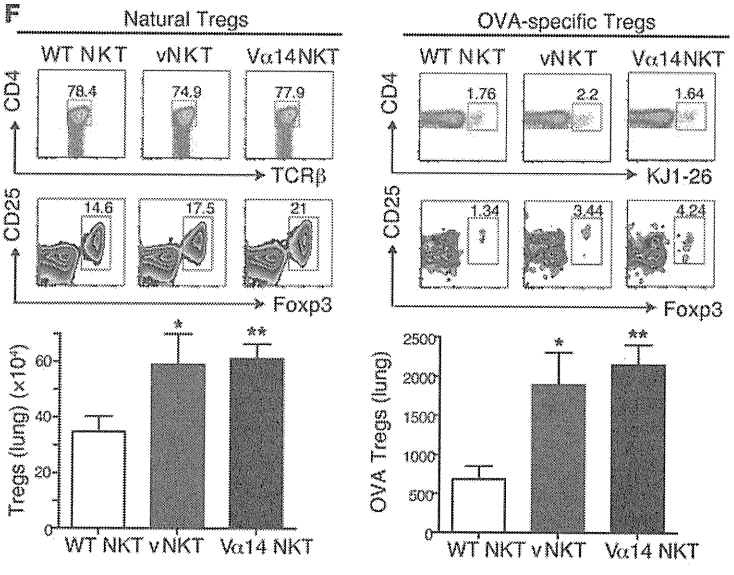
F
Natural Tregs
OVA-specific Tregs
WT NKT
vNKT
Vα14NKT
CD4
TCRβ
KJ1-26
CD25
Foxp3
78.4
74.9
77.9
14.6
17.5
21
1.76
2.2
1.64
1.34
3.44
4.24
Tregs (lung) (×10⁴)
OVA Tregs (lung)
WT NKT vNKT Vα14 NKT

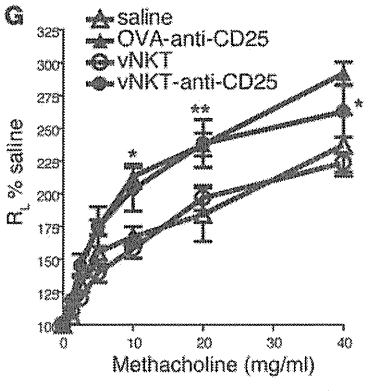
G
saline
OVA-anti-CD25
vNKT
vNKT-anti-CD25
R_L % saline
Methacholine (mg/ml)

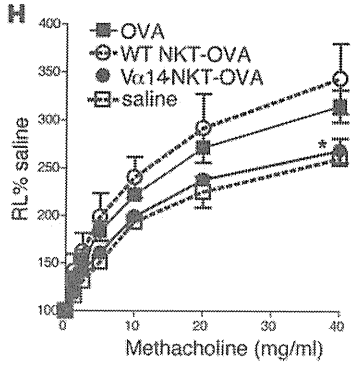
H
OVA
WT NKT-OVA
Vα14NKT-OVA
saline
RL% saline
Methacholine (mg/ml)

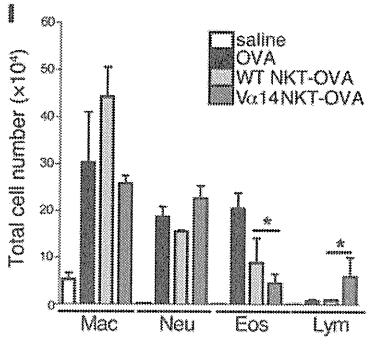
I
saline
OVA
WT NKT-OVA
Vα14NKT-OVA
Total cell number (×10⁴)
Mac
Neu
Eos
Lym

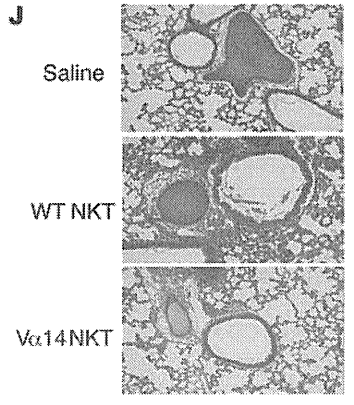
J
Saline
WT NKT
Vα14NKT

Figure 4
H3N1-exposed NKT cells suppress AHR and increase OVA-specific Tregs. (**A**) Protocol for adoptive transfer of NKT cells. (**B** and **C**) Lung resistance was measured in recipient mice (**B**; $n = 15$/group) and BAL cells collected (**C**). (**D**) Relative numbers of $CD4^+$ versus DN NKT cells in recipients' lungs were assessed (**E**) H3N1-exposed $CD4^-CD8^-$NKT (vDN NKT) or $CD4^+$NKT (vCD4 NKT) cells were purified and transferred as in **A**. Lung resistance was measured in recipient mice ($n = 5$/group). (**F**) Eight-week-old WT BALB/c mice received 5×10^4 DO11.10 *Rag*$^{-/-}$ T cells and were sensitized with OVA/alum. Seven days later, NKT cells from WT BALB/c, Vα14tg, or H3N1-infected mice were adoptively transferred into OVA-sensitized mice. After OVA challenge, the numbers of natural Tregs ($CD4^+C25^+Foxp3^+$) and adaptive OVA antigen–specific Tregs ($CD4^+$ $CD25^+$ $Foxp3^+KJ1\text{-}26^+$) were determined. Absolute cell numbers were calculated ($n = 5$/group). (**G**) Eight-week-old WT BALB/c recipients were depleted of Tregs through injections of anti-CD25 mAb (clone PC61; 0.5 mg) and assessed as in **A** ($n = 5$/group). (**H** and **I**) NKT cells from WT or Vα14 Tg were transferred to OVA-sensitized BALB/c mice ($n = 4$–6/group), which were assessed as in **A** (**H**), and BAL cells were analyzed (**I**). (**J**) Representative lung sections from recipients described in **H** were H&E stained (original magnification, ×10). Data represent 2–3 independent experiments. $^*P < 0.05$, $^{**}P < 0.01$, $^{***}P < 0.001$ versus WT NKT-OVA (**B**–**D**), OVA (**E**), WT NKT (**F**, **H**, and **I**), and OVA-vNKT (**G**).

As noted above (Figure 3F), protection against AHR was associated with an increase in the number of DN NKT cells following H3N1 infection in WT mice, which did not occur in *Tlr7*$^{-/-}$ or *Tbet*$^{-/-}$ mice (Figure 5D). Moreover, adoptive transfer of NKT cells purified 6 weeks after H3N1 infection of WT, but not *Tlr7*$^{-/-}$ or *Tbet*$^{-/-}$ mice, into OVA-sensitized WT BALB/c mice suppressed OVA-induced AHR and airway inflammation (Figure 5, E and F). Taken together, these results indicate that protection by H3N1-exposed NKT cells against AHR depends on TLR7 and T-bet.

Induction of protection with α-C-GalCer and a glycolipid from H. pylori. Since NKT cells appeared to mediate the effects of H3N1 infection, we examined a panel of glycolipids that specifically activate NKT cells for the capacity to replicate the beneficial effects of H3N1 infection. We first examined the effects of α-C-GalCer, a synthetic C-glycoside analog of α-GalCer that preferentially induces IFN-γ but not IL-4 synthesis (25–27). Treatment of suckling mice with α-C-GalCer (5 μg), but not α-GalCer, which induces production of both IFN-γ and IL-4, protected the mice as adults (42 days later) from the development of OVA-induced AHR (Figure 6A). The protective effect was dependent on T-bet, since *Tbet*$^{-/-}$ mice were not protected by treatment with α-C-GalCer (Figure 6B). Moreover, adoptive transfer of NKT cells exposed to α-C-GalCer protected recipients against the development of AHR and airway inflammation (Figure 6C).

We also found a second glycolipid, PI57, a cholesterol-derived lipid from *H. pylori* (28), that could protect against the development of AHR (Figure 6D). *H. pylori*, a bacteria that colonizes the stomach (29) and is associated with protection against asthma (2, 3), produces cholesteryl α-glucosides (30), including cholesteryl 6-O-acyl α-glucoside (AGlc-Chol) (Supplemental Figure 4), which was chemically synthesized (PI57) (Figure 6D). PI57, when administered i.p. to 2-week-old mice, increased the total number of NKT cells, particularly the number of DN NKT cells, found in the lung 2 weeks later (Figure 6, E and F). In contrast, treatment with α-GalCer increased both $CD4^+$ and DN NKT cells in the lungs. Importantly, treatment of 2-week-old mice with PI57 (50 or 100 μg) (Figure 6G) protected the mice from the development of OVA-induced AHR, induced 6 weeks after the glycolipid treatment. On the other hand, treatment of 2-week-old mice with PBS30, a lipid present in the cell walls of *Sphingomonas* bacteria (31, 32), failed to protect the mice from OVA-induced AHR (Figure 6H). Moreover, adoptive transfer of NKT cells from PI57-treated, but not vehicle-treated, 2-week-old mice (harvested 6 weeks after treatment) into OVA-sensitized WT mice, suppressed AHR and airway inflammation (Figure 6, I and J). Transfer of NKT cells from α-GalCer–treated mice reduced AHR slightly, but this was not statistically significant (Supplemental Figure 3A). The production of IFN-γ by the NKT cells was important, since the protective effect of PI57, like that of H3N1 and α-C-GalCer, was dependent on T-bet, since PI57 treatment of 2-week-old *Tbet*$^{-/-}$ mice did not protect against subsequent OVA-induced AHR (Supplemental Figure 3B). These results together suggest that a subset of NKT cells that can be specifically activated by some but not all glycolipid antigens, and that preferentially produces IFN-γ, mediates the protective effects of H3N1 infection.

PI57 is a CD1d-dependent NKT cell antigen. To demonstrate that PI57, like α-C-GalCer, can directly activate NKT cells, we showed that PI57, when added to cultures of NKT cell lines plus DCs, induced the production of IFN-γ in a CD1d-restricted manner, since cytokine production was blocked by anti-CD1d mAb (Figure 7A). In addition, PI57 induced higher levels of IFN-γ and less IL-4 in NKT cell lines compared with PBS30 (from *Sphingomonas*) or α-GalCer, and did so in a CD1d-restricted manner, since DCs from *Cd1d*$^{-/-}$ mice failed to support PI57-induced cytokine production (Figure 7B). Furthermore, the PI57 response occurred by direct activation of NKT cells, since PI57 induced cytokine production in NKT cell lines with DCs from *Myd88*$^{-/-}$ or *Trif*$^{-/-}$ mice (Figure 7B), and since 3 different NKT cell hybridomas derived from Vα14 NKT cells but not from $V\alpha14^-$ T cells produced IL-2 in response to immobilized recombinant CD1d previously loaded with PI57 but not with PI56, a control glycolipid (Figure 7C). Moreover, CD1d tetramers loaded with PI57 stained 10%–23% of NKT cells in an NKT cell line (Figure 7D). Of the PI57-CD1d tetramer$^+$ cells, 92% were $CD4^-$ (DN) (data not shown). This strongly suggests that PI57 bound to CD1d was directly recognized by the TCR of a population of NKT cells. Finally, human NKT cells were also activated by PI57, since NKT cells lines (Figure 7E) as well as a $V\alpha24^+$ NKT cell clone (BM2a.3) (Figure 7F) responded to this glycolipid. The response was also directly induced, since plate-bound CD1d loaded with PI57 induced IFN-γ in BM2a.3 cells (Figure 7G). Taken together, these results indicated that both mouse and human NKT cells were directly activated by PI57, an *H. pylori* glycolipid, in a CD1d-restricted manner.

Discussion

Herein, we showed that infection of 2-week-old pups with influenza A virus H3N1 protected against the subsequent development of allergen-induced AHR, whereas infection of adult (8-week-old) mice with H3N1 did not protect against the subsequent development of AHR. The protective effect H3N1 in suckling mice was associated with the maturation and expansion of a specific subset of NKT cells, which suppressed the development of allergen-induced AHR, demonstrated by adoptive transfer of these NKT cells into normal allergen-sensitized adult mice. The protective NKT cell subset required T-bet, as the NKT cells had to be derived from T-bet$^+$ mice; this subset also produced IFN-γ and was present in NKT cell populations enriched for DN ($CD4^-$) NKT cells. Adoptive transfer of the protective NKT cell population was associated

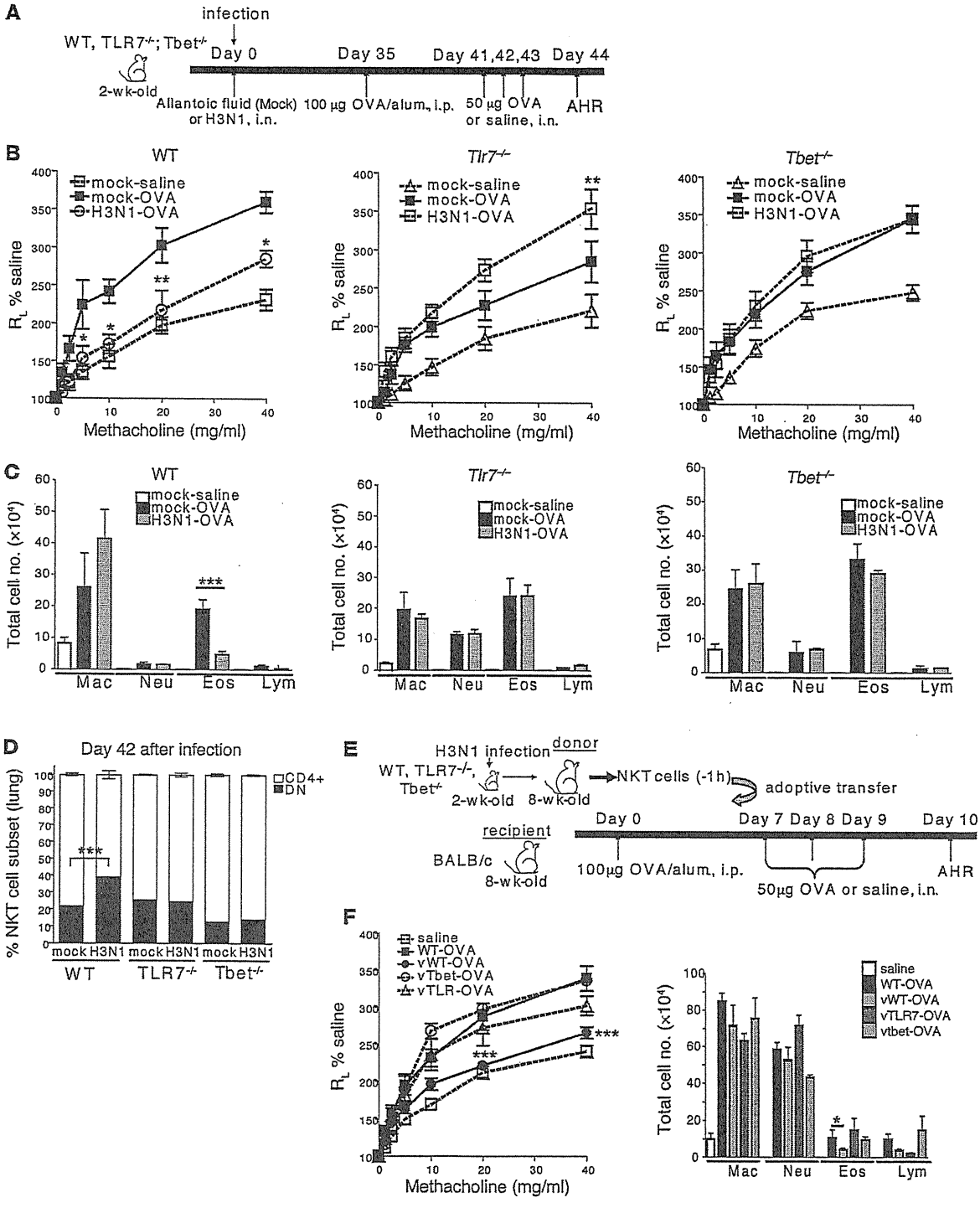

Figure 5

The protective effect of H3N1 infection depends on TLR7 and T-bet. (**A**) Schematic showing the protocol for WT, *Tlr7*$^{-/-}$, or *Tbet*$^{-/-}$ mice infected at 2 weeks of age with H3N1 virus or mock infected and examined for OVA-induced AHR at 8 weeks of age ($n = 4$–6 per group). (**B**) Lung resistance was measured. $^{*}P < 0.05$, $^{**}P < 0.01$, $^{***}P < 0.001$ compared with the mock-OVA group. (**C**) BAL cells from **B** were collected. (**D**) WT, *Tlr7*$^{-/-}$, or *Tbet*$^{-/-}$ mice were infected with H3N1 or mock at 2 weeks of age, and lung samples were taken 42 days later to asses for NKT cell subsets. $^{***}P < 0.001$ compared with the mock group. (**E**) Schematic showing the adoptive transfer of NKT from virus-infected WT, *Tlr7*$^{-/-}$, or *Tbet*$^{-/-}$ mice to OVA-sensitized BALB/c recipients ($n = 4$–6 per group). The donor mice were infected with H3N1 or mock-infected at 2 weeks of age. NKT cells were purified from these mice 42 days after infection and transferred to OVA-sensitized BALB/c mice, which were then challenged with OVA to induce AHR. (**F**) Left: After OVA challenge, AHR was measured as described in **D**. Right: Cells in BAL were assessed. $^{***}P < 0.001$ compared with the WT-OVA group. Data are representative of 2 independent experiments.

with the expansion of allergen-specific Foxp3$^+$ Treg cells, suggesting that the suppressive effect was mediated by Foxp3$^+$ Treg cells. Moreover the protective effect of H3N1 infection could be replicated by treating suckling mice with NKT cell–activating glycolipids from *H. pylori* or with α-C-GalCer. These studies are particularly important not only because they characterize an NKT cell population that suppresses AHR, but also because they provide a plausible mechanism for the hygiene hypothesis and for epidemiological studies indicating that infection with respiratory viruses (9) and *H. pylori* (2, 3) protect against the development of asthma.

NKT cells comprise a small subset of T lymphocytes that share characteristics with NK cells and conventional T cells, with potent functions in modulating immunity that have only recently become appreciated (33). NKT cells express a relatively unique transcription factor, PLZF, specific for NKT cells (34) and other innate or activated T cells (35), and an invariant TCR, Vα14Jα18 in mice and Vα24 in humans, and are restricted by the MHC class I-like molecule, CD1d. The conservation of this invariant TCR across many mammalian species suggests that it is a pattern recognition receptor, and that NKT cells play an important role in innate immunity. Activation of NKT cells through this invariant TCR results in the rapid production of large amounts of cytokines, including IL-4 and IFN-γ, particularly from mature NKT cells found in adult mice and humans. In contrast, NKT cells in neonates or in cord blood are immature, and produce only small amounts of cytokines (36, 37). Nevertheless, the ability of mature NKT cells to rapidly produce very large quantities of cytokines endows that NKT cell with the capacity to play very important regulatory roles in autoimmunity, cancer, asthma, and infectious diseases (38).

NKT cells participate in immune responses to a growing list of infectious microorganisms, driven either by direct TCR recognition of specific glycolipids expressed by microorganisms, as in the case of *Borrelia burgdorferI* (39) and *Sphingomonas paucimobilis* (32, 40), or by indirect responses to cytokines released by activated DCs, as in the case of *Salmonella typhimurium* (41), *E. coli*, *Staphylococcus aureus*, *Listeria monocytogenes* (42), and *Mycobacteria tuberculosis* (43, 44). During influenza A infection in adult mice, NKT cells abolished the suppressive activity of influenza A–induced myeloid-derived suppressor cells, thereby enhancing survival (18). Our current studies also suggest that NKT cells may respond during infection with influenza A, and to glycolipids (PI57) produced by *H. pylori*, resulting in inhibitory effects on immunity, though primarily in young mice. The capacity of *H. pylori* glycolipids to activate a regulatory NKT cell subset (but only in young mice) may also explain the protective effects of *H. pylori* infection in neonatal but not older mice against gastritis and malignant metaplasia (45) as well as the observation that only WT, and not cholesterol-α-glucosyltransferase–deficient, *H. pylori* can infect the gastric mucosa of mice (28), given that cholesterol-α-glucosyltransferase is required for synthesis of PI57 (46). Finally, we would like to point out that the structure and function of PI57 is unique, since it includes a cholesterol-containing tail distinct from previously described NKT cell ligands, and since it represents the first demonstration of cholesterol as a target for TCR recognition.

NKT cells thus react to a diverse group of pathogens by functioning as an innate immune cell that can sense and rapidly respond to the presence of infectious agents. The capacity to respond to such pathogens, however, may be limited in neonates and young children due to limited numbers and to the immaturity of NKT cells (36, 37). On the other hand, the immaturity of NKT cells in young children may provide an opportunity for infection and therapeutic intervention to influence the subset composition of NKT cells, thereby preventing the development of asthma and allergy.

In asthma, NKT cells have been suggested to play a very important pathogenic role (20, 47). This idea has become controversial, since some patients, particularly those with mild or well-controlled asthma, have few detectable pulmonary NKT cells, although patients with severe or poorly controlled asthma have a significant increase in pulmonary NKT cells (19, 48, 49). Nevertheless, in many distinct mouse models of asthma, the presence of specific NKT cell subsets was required for the development of AHR. For example, CD4$^+$IL-17RB$^+$ NKT cells are required in allergen-induced AHR (19, 20, 50, 51); in ozone-induced AHR, an NK1.1$^-$ IL-17–producing subset is required (21); and in Sendai virus–induced AHR, a CD4$^+$ NKT cell population that interacts with alternatively activated alveolar macrophages is required (22). While previous studies have suggested that some (DN) NKT cells could not induce AHR (50), we now show for the first time that a population of NKT cells, enriched for a DN, T-bet–dependent, and IFN-γ–producing subset, has a potent regulatory role, suppressing the development of AHR. Although previous studies have suggested an inhibitory role for NKT cells in asthma, since adoptive transfer of NKT cells acutely activated with α-GalCer (1 hour prior to transfer) inhibit the development of experimental asthma in a C57BL/6 mouse model (52), we believe that our current studies are quite distinct. We showed that H3N1 infection in suckling mice expanded a population of NKT cells that, when examined 42 days after infection, specifically suppressed allergen-induced AHR without the need for acute activation with exogenous glycolipids.

While H3N1 infection affects many different cell types, the fact that the protective effect of H3N1 infection could be transferred with purified NKT cells, and the fact that the protective effect could be replicated by treatment of suckling mice with α-C-GalCer or a glycolipid from *H. pylori* (PI57) that specifically activated NKT cells in a CD1d-restricted fashion, strongly suggests that the protective effect of H3N1 infection in young mice was primarily mediated by a subset of NKT cells. The NKT cell subset activated by PI57 in suckling mice appeared to be a subset of invariant NKT cells, since DN NKT cells in suckling mice expanded after treatment with PI57, and since CD1d tetramers loaded with PI57 could stain NKT cells. The precise mechanism by which the DN NKT cells suppressed AHR is not clear, but may involve the preferential production of IFN-γ but not IL-4, since DN NKT cells from H3N1-infected suckling *Tbet*$^{-/-}$ mice failed to inhibit AHR. A role for IFN-γ is also supported by our observation that treatment of suckling mice with α-C-GalCer, which preferentially induces IFN-γ (26), also prevented the development of OVA-induced AHR 42 days later, whereas treatment with α-GalCer or with *Sphingomonas* glycolipid (PBS30) did not.

The "regulatory" NKT cells mediating the inhibitory effect of H3N1 and of PI57 and α-C-GalCer may be similar to previously described DN NKT cells that protected against the development of type I diabetes in humans and in mice (53, 54), to IFN-γ–producing NKT cells that were required for allograft tolerance (55), or to IL-4–producing NKT cells that induced Treg cells in the prevention of graft versus host disease (56–58). In our experiments, increased numbers of both natural and adaptive OVA-specific Treg cells were associated with the regulatory NKT cells and were blocked by treatment with anti-CD25 mAb (Figure 4, F and G). Moreover, we believe that our studies are the first to demonstrate the existence of a

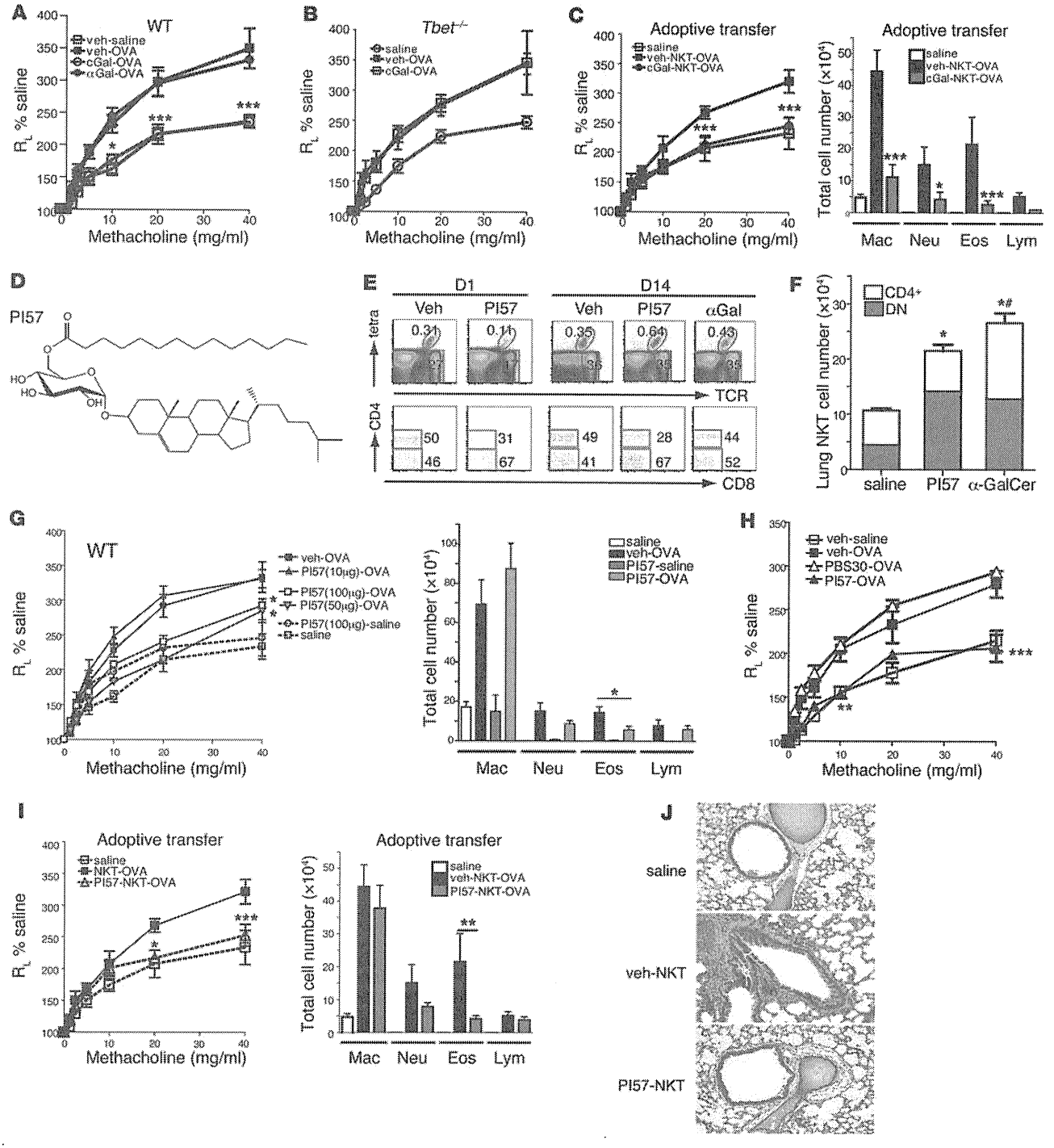

Figure 6

Induction of protection with α-C-GalCer and a glycolipid from *H. pylori*. (**A**) Two-week-old BALB/c mice ($n = 6–8$/group) or (**B**) *Tbet*$^{-/-}$ mice ($n = 4–6$ per group) received 5 μg α-GalCer (cGal), 2 μg α-GalCer, or vehicle. After OVA sensitization and challenge, AHR was measured on day 44. (**C**) Donor mice were treated with α-C-GalCer (5 μg) or vehicle i.p. NKT cells served as donors, as in Figure 4A ($n = 4$ per group). Lung resistance (left) and cell counts in BAL (right) were assessed. (**D**) Structure of PI57. (**E**) Mice received PI57 (50 μg), α-GalCer (2 μg), or vehicle i.p., and lungs were examined 1 or 14 days later for CD4 and CD8 expression. (**F**) Absolute numbers of CD4$^+$ NKT and DN NKT subsets from E were assessed. (**G**) BALB/c mice ($n = 5–8$/group) received PI57 or vehicle i.p. Lung resistance (left) and BAL cells (right) were assessed. (**H**) BALB/c mice treated with PI57 (50 μg), PBS30 (*Sphingomonas* glycolipid) (50 μg), or vehicle i.p. were assessed for AHR as in **G**. (**I**) Donor mice were treated with PI57 (50 μg) or vehicle i.p. NKT cells served as donors as in Figure 4A. Lung resistance (left) and BAL cells (right) were assessed ($n = 4$ per group). (**J**) Representative lung sections from I stained with H&E (original magnification, ×10). Data represent 2–3 independent experiments. $^*P < 0.05$, $^{\#}P < 0.05$, $^{***}P < 0.001$ versus vehicle-OVA (**C**, **G**, and **I**), DN NKT saline (**F**), and CD4$^+$ NKT saline (**F**).

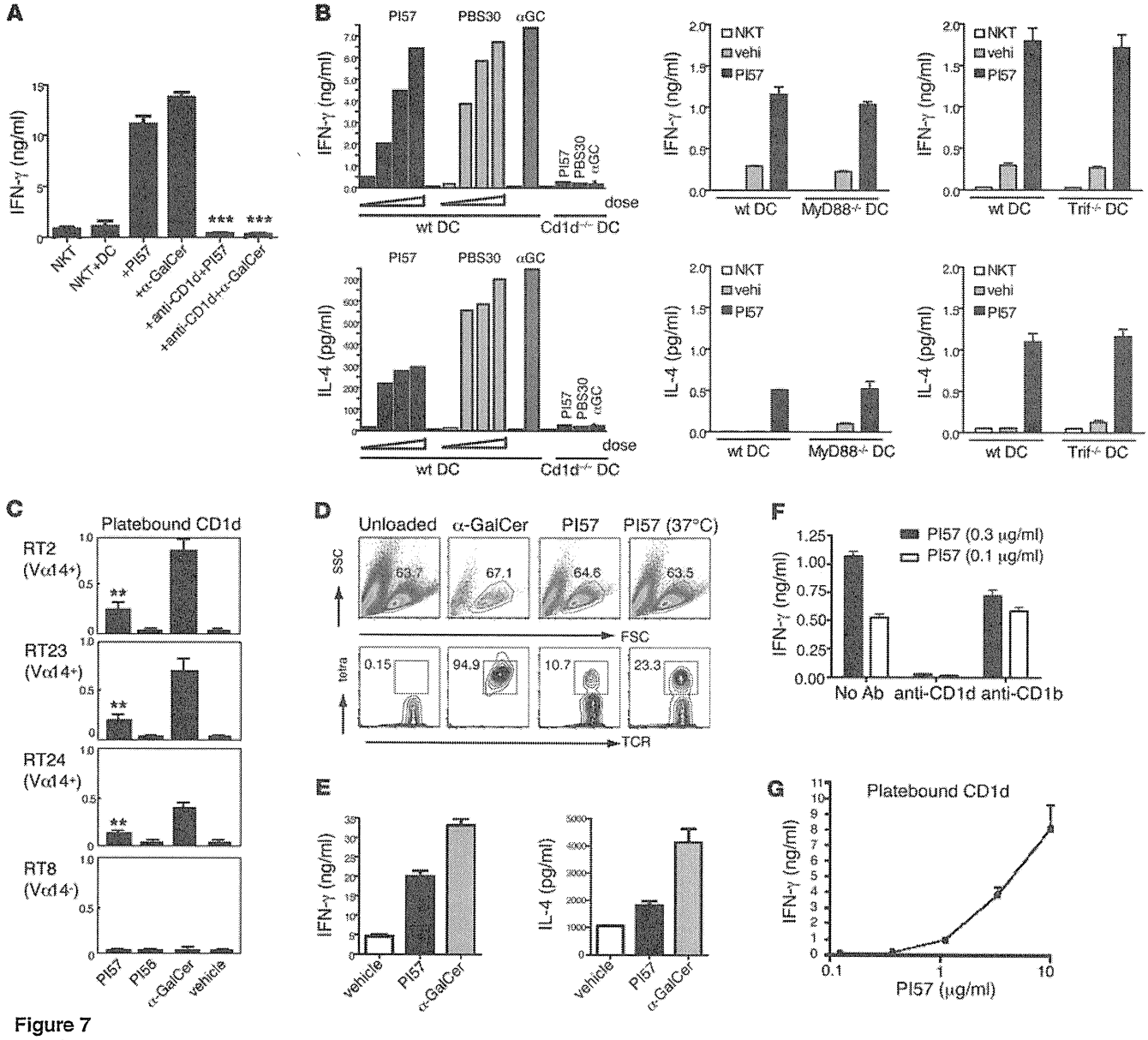

Figure 7

PI57 directly activates NKT cells. (**A**) NKT cell lines were cocultured with BM-derived DCs (BMDCs) and α-GalCer (100 ng/ml), PI57 (10 μg/ml), or vehicle for 48 hours, with or without pre-incubation with anti-CD1d (10 μg/ml). IFN-γ was measured by ELISA. (**B**) Murine NKT cell lines were cocultured as in A with BMDCs from WT, *Cd1d*$^{-/-}$, *Myd88*$^{-/-}$, or *Trif*$^{-/-}$ mice. Cells were treated with α-GalCer (100 ng/ml), PI57 (2.5, 5, or 10 μg/ml), PBS30 (1, 2.5, or 5 μg/ml), or vehicle for 48 hours. IFN-γ and IL-4 were measured by ELISA. (**C**) IL-2 production from hybridomas derived from invariant Vα14 NKT cells (RT2, RT23, and RT24) and an irrelevant Vβ8$^+$ T cell (RT8; control) (see Supplemental Methods). (**D**) Mouse NKT cell lines were stained with PE-labeled CD1d tetramers of PI57 or α-GalCer at 4°C for 45 minutes or 37°C for 25 minutes, and with anti-TCRβ–APC antibody. Top: Lymphocytes were gated in the FSC/SSC window. Bottom: Percentage of CD1d tetramer$^+$ cells. (**E**) IFN-γ and IL-4 production from human NKT cell lines by treatment with α-GalCer (100 ng/ml), PI57 (10 μg/ml), or vehicle for 48 hours in vitro (see Supplemental Methods). (**F**) IFN-γ production from CD1d-transfected NKT cell clone BM2a.3 in presence of PI57 and blocking mAb against human CD1d or CD1b (see Supplemental Methods). (**G**) CD1d Fc-coated Maxisorp plates were loaded with lipid and cultured with 5 × 10^4 NKT cells. IFN-γ was analyzed by ELISA after 24 hours. Data represent 3 or 5 independent experiments.

subpopulation of NKT cells that can suppress the effects of other subpopulations of NKT cells that enhance the development of experimental asthma. These results suggest that a balance exists between NKT cells that induce, and those that protect against, AHR, and that stimulation with H3N1, α-C-GalCer, or *H. pylori* glycolipids, but not a *Sphingomonas* glycolipid or α-GalCer, may selectively expand this regulatory NKT cell population in young mice. The inability of α-GalCer to protect may be due to the fact that it nonselectively stimulates all invariant NKT cells or because it may anergize NKT cells, including suppressive populations. Nevertheless, these data support the idea that under normal, pathogen-free conditions, CD4$^+$ NKT cells that induce AHR predominate, but that in very young mice, exposure to Th1-skewing reagents that can alter the composition of NKT cell subpopulations may change subsequent lung immunity.